

5-1-2013

Closed Loop Control of a Cylindrical Tube Type Ionic Polymer Metal Composite (IPMC)

Benjamin Mead

University of Nevada, Las Vegas, meadb@unlv.nevada.edu

Follow this and additional works at: <https://digitalscholarship.unlv.edu/thesesdissertations>



Part of the [Biomaterials Commons](#), [Biomechanical Engineering Commons](#), [Biomedical Commons](#), [Biomedical Devices and Instrumentation Commons](#), [Materials Science and Engineering Commons](#), and the [Medical Biotechnology Commons](#)

Repository Citation

Mead, Benjamin, "Closed Loop Control of a Cylindrical Tube Type Ionic Polymer Metal Composite (IPMC)" (2013). *UNLV Theses, Dissertations, Professional Papers, and Capstones*. 1861.
<https://digitalscholarship.unlv.edu/thesesdissertations/1861>

This Thesis is protected by copyright and/or related rights. It has been brought to you by Digital Scholarship@UNLV with permission from the rights-holder(s). You are free to use this Thesis in any way that is permitted by the copyright and related rights legislation that applies to your use. For other uses you need to obtain permission from the rights-holder(s) directly, unless additional rights are indicated by a Creative Commons license in the record and/or on the work itself.

This Thesis has been accepted for inclusion in UNLV Theses, Dissertations, Professional Papers, and Capstones by an authorized administrator of Digital Scholarship@UNLV. For more information, please contact digitalscholarship@unlv.edu.

CLOSED LOOP CONTROL OF A CYLINDRICAL TUBE TYPE IONIC POLYMER
METAL COMPOSITE (IPMC)

By

Benjamin T Mead

Bachelor of Science in Engineering
Calvin College
2007

A thesis submitted in partial fulfillment
of the requirements for the

Master of Science in Mechanical Engineering

Department of Mechanical Engineering
Howard R. Hughes College of Engineering
The Graduate College

University of Nevada, Las Vegas
May 2013



THE GRADUATE COLLEGE

We recommend the dissertation prepared under our supervision by

Benjamin T. Mead

entitled

Closed Loop Control of a Cylindrical Tube Type Ionic Polymer Metal Composite (IPMC)

be accepted in partial fulfillment of the requirements for the degree of

Master of Science in Mechanical Engineering

Department of Mechanical Engineering

Woosoon Yim, Ph.D., Committee Chair

Brendan O'Toole, Ph.D., Committee Member

Mohamed Trabia, Ph.D., Committee Member

Sahjendra N. Singh, Ph.D., Graduate College Representative

Tom Piechota, Ph.D., Interim Vice President for Research &
Dean of the Graduate College

May 2013

ABSTRACT

CLOSED LOOP CONTROL OF A CYLINDRICAL TUBE TYPE IONIC POLYMER METAL COMPOSITE (IPMC)

By

Ben Mead

Dr. Woosoon Yim, Examination Committee Chair

Professor of Mechanical Engineering

University of Nevada, Las Vegas

The goal of this research is to provide a framework for the integration of tube type, cylindrical Ionic Polymer Metal-Composite (IPMC) into conventional devices. IPMCs are one of the most widely used types of electro-active polymer actuator, due to their low electric driving potential and large deformation range. For this research a tube type IPMC was investigated. This IPMC has a circular cross section with four separate electrodes on its surface and a hole through the middle. The four electrodes allow for biaxial bending and accurate control of the tip location. One of the main advantages of using this type of IPMC is the ability to embed a specific tool and accurately control the tool tip location using the large deflection range of the IPMC. This ability has widespread applications including in the biomedical field for use in active catheter procedures.

First, this relatively new type of IPMC is investigated and characterized. The processes and materials used are described and the functional design is explored. Before

the modeling process beings the basic functions of the IPMC are investigated. To this end force and displacement experiments are performed to describe the activation of the tube type IPMC. This data will be used later to verify and calibrate the mathematical simulations.

Second, a three dimensional multi-physics finite element model is developed using COMSOL 4.3a. This model will automatically couple three physics packages and provide a description of the fluid interactions within the tube type IPMC. This model is then compared against the experimental displacement results to calibrate the simulation. Using this simulation design parameters are declared including, overall diameter, and tool hole size. The performance of the IPMC is then simulated while varying these parameters.

Third, an electro-mechanical model of the IPMC is developed. This macroscopic model is used to relate the input voltage to an associated tip deflection. Several model types used for this purpose are tested and discussed. After determining a suitable type a mathematical electro-mechanical model is developed. Using this model several closed loop control systems are proposed. Once a final decision is reached the closed loop control system is implemented in the experimental setup. Several tests are designed to test the effectiveness of the closed loop system and mathematical models.

Finally several improvements are made to enhance the users experience using IPMCs as well as incorporating them into conventional devices. To provide a better user interface the experimental control system is extended to allow the user to input controls via a standard computer mouse. This will allow a shorter operator training time and

hopefully a wider array of real world uses for IPMCs. Attempts are also made to establish permanent connections to the IPMC. A tube type IPMC is meant to be used as part of a total system. To this end soldered connections to the IPMC are made. One of the main expected applications of tube type IPMCs are as active catheters. In this application the IPMC would be placed in-line with the plastic catheter line. As a proof of concept the IPMC is installed onto the tip of a conventional catheter line.

ACKNOWLEDGMENTS

I would like to thank my advisor Professor Woosoon Yim for all of his guidance and advice. I would like to thank everyone on my committee Professor Trabia, Professor O'Toole, and Professor Singh for putting up with all of my emails and taking the time to read my thesis. I would like to thank Joan from the mechanical engineering office for steering me through all of the necessary forms. I am grateful to Siul Ruiz for being a most excellent research partner and an excellent person to bounce ideas off of. I would like to thank Eldon Goddard for his help in setting up many of my experiments. I am extremely grateful to Mr. Richard Jennings for his help soldering to the IPMC in addition to all of his real world knowledge and experience.

I would like to thank Professor Kwang Kim and Viljar Palmre from the University of Nevada, Reno for producing and providing the IPMC samples. I would like to thank David Pugal for reviewing the models and for being an excellent technical resource. I would like to thank Shivakanth Gutta for laying the IPMC groundwork at UNLV. .

I gratefully acknowledge the support of the National Science Foundation (Award No. 0958565). I would also like to thank my wife Laura for all of her support.

TABLE OF CONTENTS

Abstract	iii
Acknowledgments.....	vi
List of Tables	ix
List of Figures	x
Chapter 1 Introduction	1
Literature Review	3
Chapter 2 Tube Type IPMC Characterization	9
Physical Description.....	9
Fixtures.....	11
Force and Displacement Experiments.....	14
Chapter 3 Finite Element Method.....	18
Material Properties, Geometry, and Mesh	18
Mesh	21
Multi-Physics	23
Finite Element Results	27
Chapter 4 Closed Loop Control	37
Electro-Mechanical Modeling.....	37
Controller Design	46
Experimental Setup	54
Closed Loop Experiments	59
Closed Loop Results.....	62
Chapter 5 Implementation.....	70
Mouse Control.....	70

Permanent Connections.....	74
Chapter 6 Conclusion.....	79
Future Work	80
References.....	82
Curriculum Vitae	87

LIST OF TABLES

Table 1 - IPMC Sample Sizes	11
Table 2 - Comsol Parameters and Variables	20
Table 3 - Comsol Material Properties	21
Table 4 - Curve Fit Coefficients	46
Table 5 - Labview Control Elements	72

LIST OF FIGURES

Figure 1 - Basic IPMC Actuation	2
Figure 2 - Cylindrical Tube Type IPMC Description	10
Figure 3 - First Experimental Fixture IPMC	12
Figure 4 - Newest IPMC Experimental Fixture SolidWorks Model	13
Figure 5 - Electrode Contacts in Final Fixture Design	14
Figure 6 - Deflection Characterization of the Tube Type IPMC	15
Figure 7 - Force Characterization of the Tube Type IPMC	17
Figure 8 - IPMC Finite Element Model Geometry	19
Figure 9 - Tube Type IPMC Finite Element Mesh	22
Figure 10 - Finite Element Electro-Statics Boundary Conditions	24
Figure 11 - Transport of Diluted Species Boundary Conditions	25
Figure 12 - Solid Mechanics Boundary Conditions	27
Figure 13 - Electro-Statics Results	28
Figure 14 - Cation Concentration Levels	29
Figure 15 - Deformation of the Tube Type IPMC	30
Figure 16 - Simulation versus Experimental Displacement	31
Figure 17 - Constant Diameter Varied Hole Diameter Simulation	33
Figure 18 - Constant Radius Varied Hole Size Deflection Results	34
Figure 19 - Various IPMC Geometries	35
Figure 20 - Tube Type IPMC Deflection with Constant Hole Diameter	36
Figure 21 - RC Circuit Model	37
Figure 22 - Electrical Step Response of IPMC	38
Figure 23 - Sinusoidal Voltage Input IPMC	39
Figure 24 - Curvature to Displacement Conversion [25]	43
Figure 25 - Deflection Curve Fit at 1.5 Volts	45
Figure 26 - Open Loop Simulation Schematic in Matlab Simulink	47
Figure 27 - Closed Loop PI Controller	48
Figure 28 - Deflection and Voltage Simulation Data	49
Figure 29 - Maximum Displacement Correlated to Voltage	50
Figure 30 - Control Law Simulation for Steady State Voltage	51
Figure 31 - Circular Simulation with 1.5 Volt Saturation	52
Figure 32 - Simulation of circular trajectory following	53
Figure 33 - Closed Loop Control Experimental Setup	54
Figure 34 - Labview PXI-7833R FPGA Assignment	56
Figure 35 - Labview Contour Extraction VI	58
Figure 36 - Labview Image Acquisition Region of Interest	59
Figure 37 - Labview PI Block Diagram	60

Figure 38 - Experimental Circle with Radii .1 mm and .15 mm	62
Figure 39 - Experimental Circle Following Data Various Circle Sizes.....	63
Figure 40 - Simulation Versus Experimental Electrical Data.....	64
Figure 41 - Figure 8 Closed loop control verification (top) circular path follow (bottom left) x position (bottom right) y position.....	65
Figure 42 - Electrical Data from .3 mm Radius Circle Following.....	67
Figure 43 - Block Diagram Mouse Motion Control VI	71
Figure 44 - Labview User Interface	72
Figure 45 - Closed loop mouse control (top) figure 8 path follow (bottom left) x position (bottom right) y position	73
Figure 46 - Tube Type IPMC Soldering	75
Figure 47 - Manual Wire Bonding Station	76
Figure 48 - IPMC Connected to a Plastic Catheter Line	78

CHAPTER 1

INTRODUCTION

Ionic Polymer Metal Composites (IPMC) are a type of smart material known as an electro active polymer. These devices are made from an ionic polymer, typically Nafion or Flemion, coated with a highly conductive metal such as gold or platinum. IPMCs are a popular choice for many applications due to their large deflections under relatively small input voltages. This actuation is caused by the motion of charged particles within the IPMC. The ionic polymer contains anions that are fixed to the polymer backbone and mobile cations such as Na^+ , K^+ , Li^+ or Cs^+ . When an external electrical field is applied to the electrodes hydrated cations within the polymer are drawn across the IPMC. This cation motion carries along with it water molecules and other solvents. This influx of fluid to a single side of the IPMC induces a bending towards the anode. The degree of bending is proportional to the voltage applied.

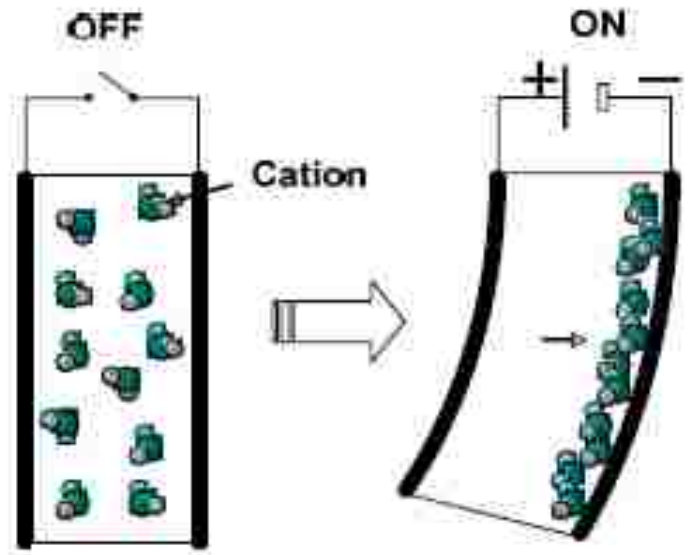


Figure 1 - Basic IPMC Actuation

This process can also be reversed causing the IPMC to be used as a sensor [1]. When an IPMC deforms the cations within the IPMC are displaced. This cation motion produces a small amount of current. This signal can then be used to measure the degree of deflection. In order to maintain the cation mobility conventional IPMCs must be kept wet. As a result most applications for IPMCs focus on aqueous environments such as robotic fish or active catheters [2, 3]. With the ability to operate both as an actuator, a sensor, and in aqueous environments IPMCs have become one of the most popular electro-active polymers.

The goal of this research is to further the potential uses of IPMCs by providing the tools to design, control, and implement a new type tube type IPMC. With additional flexibility and reliability it is hoped that tube type IPMCs can make a large contribution to society.

LITERATURE REVIEW

Most early work in IPMCs centered on the flat type IPMC. This IPMC type consists of an ionic polymer block, typically Nafion or Flemion, plated with a highly conductive metal such as platinum or gold [4, 5]. This creates a sandwich with the polymer in the middle and electrodes on the top and bottom. Several attempts have been made to increase the bending motion of the flat type IPMC. One method is to vary the plating type and the number of platings of the IPMC electrode layers [6]. Another approach is to sandwich multiple Nafion actuators together and operate them as a single actuator [7]. It has also been shown that surface treatments prior to the plating of the electrode can be effective in extending the life of the IPMC and the actuation characteristics [7].

Attempts at creating complex motion out of a flat type IPMC have also been made. The most popular method for doing so is by patterning the electrode shape. The electrode can be patterned in many ways. It can be selectively grown during the plating process [8]. Using this method the researchers were able to vary the natural frequency of the IPMC and add additional degrees of freedom to the actuator. Electrode patterns can also be developed by carefully machining the electrode surface [9]. Using this technique a twisting motion can be generated using a flat type IPMC. Electrode patterning can also be used to create a wave type motion which can oscillate and undulate [10].

The basic physics behind the deflection properties of IPMCs have been widely studied [11, 12, 13]. When modeling these properties two main approaches are developed. The first approach is to use the finite element model to describe the physics

occurring within the IPMC. Some of these models use a multi-physics approach where the fluid interactions within the IPMC are taken into account. These models take into account the actual concentration changes within the IPMC and relate the motion of these charged ions back to the overall electrical model. In this article a method for relating the local charge of the IPMC to the overall bending is established [14]. Finite element models have also used beam theory to model the bending phenomenon [15]. The model is based upon an estimation of the physical properties of the IPMC. This model establishes a force displacement relationship for the cantilevered flat type IPMC. Quite an accomplishment since few of the IPMC finite element models are able to accurately calculate the force output.

Efforts to capture the back relaxation as part of the finite element models have had some success [16]. These models are based upon the physical material properties of the IPMC however, to accurately model the forward motion and back relaxation time constants must be added to the model. These time constants require some knowledge of how the IPMC performs. The motivation behind these basic physics models is to be able to design and customized the IPMC motion and electrical characteristics. With an accurate physics model the fabrication process can be streamlined and optimized.

The second type of models being developed are the electro-mechanical models. These models use the macroscopic motion of the IPMC and the electrical inputs to correlate the voltage to an associated mechanical bending and tip deflection. The basic electrical inputs are built upon an RC circuit. The IPMC is described as a double-layer capacitor created in the boundary between the metal electrodes and the ionic polymer

[17]. This model captures the electrical input across the polymer domain however it relies upon experimental data for the model constants. The electrical response model has been improved by including a distributed RC model instead of a lumped RC model [18, 19]. This allows the capacitance and resistance to be varied along the length of the IPMC and can be modeled to more accurately reflect the electrical properties of the IPMC. This change in capacitance and resistance is due to the erratic growth of the electrodes into the polymer domain. The irregularity of this growth causes the perceived change in capacitance [18]. Several studies have been performed attempting to model this irregularity as a fractal growth of the electrode [18, 20, 21]. It is found that fractal geometry can greatly increase the accuracy of the voltage data along the length of the electrode.

The charge within the IPMC is then related to a mechanical bending force. In some cases the bending stress is correlated directly with the space charge density within the IPMC [22]. This model can accurately describe the forward motion but requires an additional stress term to account for the back relaxation. One advantage of this method is that estimates of the coefficients used can be derived from the physical properties of the IPMC. In some studies the IPMC is broken into finite element sections and the shape functions are used to relate the charge to the kinetic and potential energies [23]. This model matches the experimental data well but requires large matrix operations and tracking locations at multiple points on the IPMC. Some models have also related the electric field to an induced curvature in the IPMC [18]. The curvature is modeled with a first order ordinary differential equation. This model depends on several material

constants as well as experimentally determined time constants. It can easily be extended to include back relaxation with the addition of another set of material properties and time constants. This model tracks the experimental tip data well but has the simplification that the IPMC shape is always a perfect arc.

Most of the previous models have focused on the flat type IPMC and its specific modeling characteristics. In addition to these flat models there have been several attempts to use bi-axial bending IPMCs. Cylindrical IPMCs have been investigated and found that the tip location can be accurately controlled in two directions [24]. A three dimensional finite element deflection model for this type of IPMC is generated and tested. Other research has focused on a box type IPMC. This shape has the advantages of easily attached electrical connections and the simple separation of the electrodes [25]. In this study a manufacturing and control process for the box type IPMC is discussed.

IPMCs have a found a wide range of applications. The most common application is for the propulsion of a robotic fish [26, 27, 28]. In these applications the IPMC takes the place of a conventional motor to power the robotic fish. Guiding algorithms as well as wireless communications and environmental sensing have been developed. This area is seen as a straight forward application of the IPMC. IPMCs have also been investigated as a potential actuator in micro-pumps [29]. A proof of concept has been developed with the IPMC capable of pumping very small volumes of fluid. One of the most exciting applications of IPMCs is as an artificial muscle [30, 31, 32]. So much research has been done on this subject that there is even a book about it [33]. It is hoped that IPMCs will be instrumental in the development of soft humanoid robots.

Many of these applications have been using flat type IPMCs although biaxial bending applications have also been investigated. Circular rod type IPMCs have been used as biomimic robotic bugs [34]. Six of the rod type IPMCs are used and actuated using a stepping algorithm. This allows the bug robot to move in two directions without having to reconfigure any equipment. In this experiment specific IPMC location was not needed just the overall bending motion.

Funding for this research project was provided by the National Science Foundation in pursuit of a new smart material based active catheter. As a result the current active catheter market was investigated. Active catheters are designed to solve two major problems. The first is to be able to accurately position the catheter line inside of the human body. The second is to shield the operators from harmful radiation by operating the catheter from a distance. There are a couple of conventional materials based active catheters already available on the market. The Niobe uses embedded magnets within the catheter line and two large electro magnets to control the tip location within the patient's body [35]. There are several robotic arms that mimic the doctors motion but still use conventional catheter equipment [36] [37]. Both systems allow the doctor to operate remotely and are low cost options to the hospital. A catheter has been developed that uses telescoping concentric tubes that allows the doctor to steer each individually to maintain the necessary positions [38].

All of these systems use conventional technologies to create solutions however there are a few smart material solutions available. John D. Madden has done some work using a single degree of freedom conducting polymer to act as an active catheter [39].

Shape memory alloys have also been used to create active catheters [40]. This system uses a flexible central beam with four SMA actuators surrounding it. These actuators act as tendons capable of deflecting the tip and controlling its location. With the development of a design and control method for tube type IPMCs it is hoped that they will soon be competing in the world of smart catheterization.

CHAPTER 2

TUBE TYPE IPMC CHARACTERIZATION

PHYSICAL DESCRIPTION

The tube type IPMC was developed by Dr. K. J. Kim and his coworkers at the University of Nevada, Reno using a proprietary method [41]. The IPMC is made up of a cylindrical Nafion core with a circular hole through the middle. This hole allows the IPMC to be used for the insertion of specialized tools, utilities, and/or the administration of fluids to very specific locations. The cylindrical shape allows the IPMC to be used in areas such as active catheters where the conventional tip would be replaced by an electro-active polymer.

The Nafion core is surrounded by four sectioned, chemically plated platinum electrodes. The separation of the electrodes allows for complex electrical activations causing biaxial bending. This bending allows the tip of the tube type IPMC to be controlled in two directions.

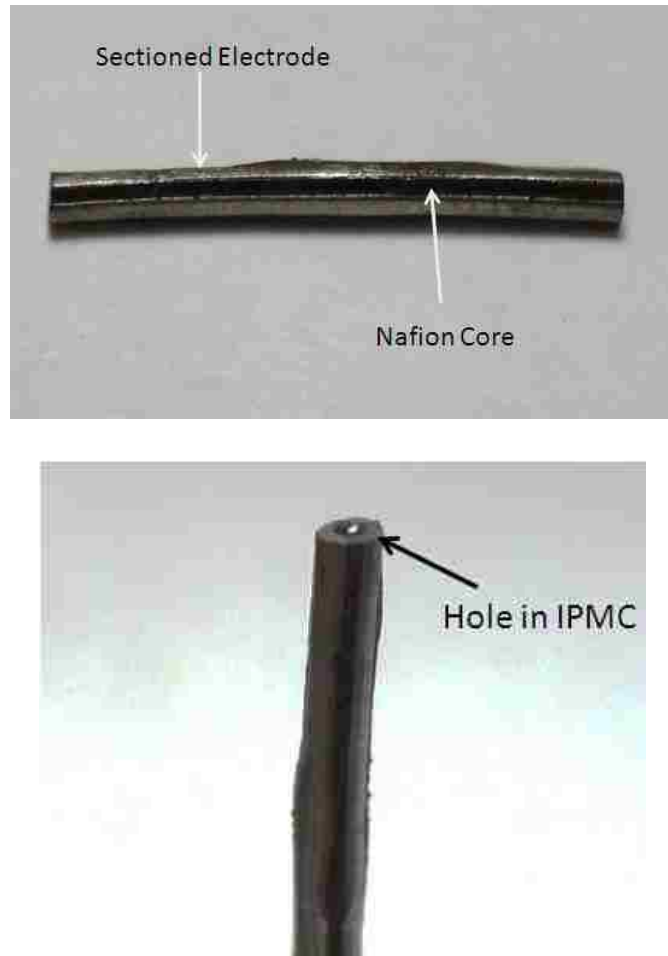


Figure 2 - Cylindrical Tube Type IPMC Description

In this research several different samples were used each with slightly different dimensions. These inconsistencies cause the samples to behave in slightly different ways. This can also be seen in flat type IPMCs where varying deflection results can be found between IPMCs with nearly identical dimensions [25]. This is the result of the complex manufacturing process and possible imperfections found in the starting materials. The deflection characteristics of IPMCs have also been found to change over time. With time smaller and smaller deflections are seen and higher voltages are needed to maintain the

same IPMC performance. With tube type IPMCs these potential problems are compounded. The isolation gaps between electrodes are difficult to produce and are often done by hand. This can produce an irregular electrode shape which will also influence how an individual IPMC performs. As a result of the variance in manufacturing and sample dimensions, each sample has a unique deflection curve and must therefore be studied individually.

Table 1 - IPMC Sample Sizes

Sample	Length (mm)	Outer Diameter (mm)	Inner Diameter (mm)
1	20.70	1.94	.94
2	23.48	1.52	.83
3	23.23	1.84	.93

FIXTURES

In order to begin modeling the motion of the tube type IPMC the bending characteristics are explored. For the experiments a specialized fixture was needed to secure the IPMC and allow for the individual activation of the four electrodes. Throughout the experiments several fixture designs were tested. The first design was a 3D printed plastic box with four compartments. These compartments were filled with a conductive silver epoxy and allowed to cure. The center of the box was drilled out with a 1 mm drill exposing four electrodes. Each electrode was machined into an arc of approximately .85 mm in length. This design although functional did not allow for variations in the IPMC diameter or inconsistencies in the electrode shape.

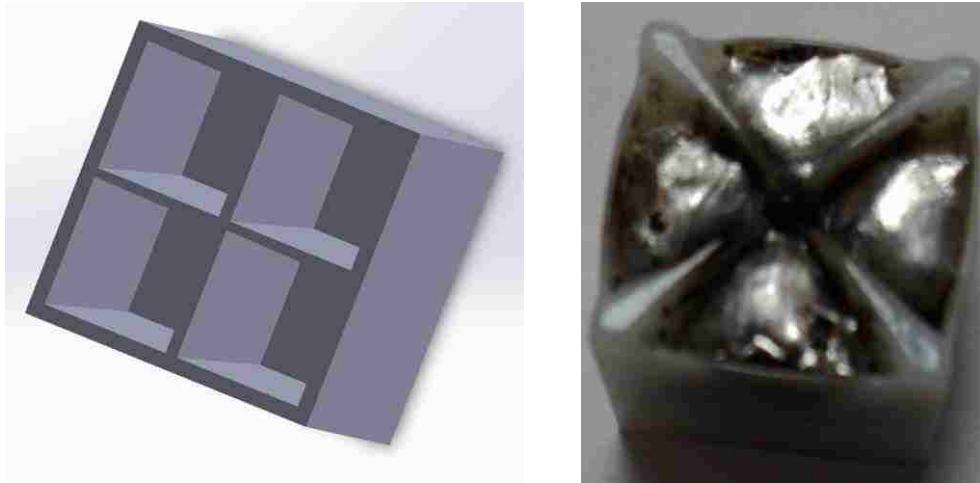


Figure 3 - First Experimental Fixture IPMC

The second design improved upon the previous concepts by splitting the single fixture in half forming two, three centimeter long rods. These rods each have a half circle in the middle sized to be slightly smaller in diameter than the tube type IPMC. With the difficulty of establishing consistent electrodes using silver epoxy small solid core wires were used instead. The wire chosen was a #24 solid core copper wire with a diameter of .40 mm. This size wire allowed for sufficient contact area with the IPMC and the flexibility to overcome inconsistencies in the IPMC electrode pattern. These wires were installed inside of the half circle clamp area in small channels that hold the wire in place. Using this design the IPMC is held securely and the separation between the four electrodes is maintained.

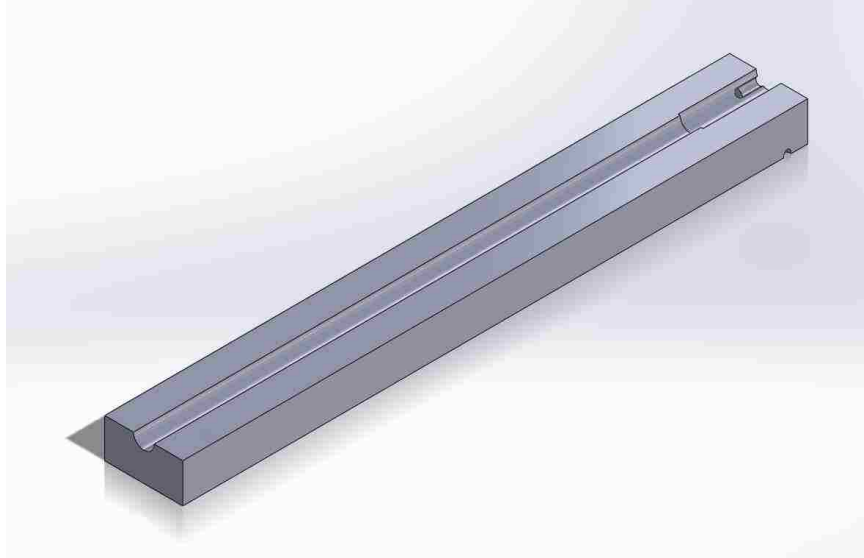


Figure 4 - Newest IPMC Experimental Fixture SolidWorks Model

This design was later improved by the addition of a channel through the base of the plastic fixture. This allowed experiments to be run with several materials placed in the middle of the IPMC. With the channel through the bottom of the fixture the IPMC did not have to be removed in-between experiments. This channel was also used for the installation of a central ground.



Figure 5 - Electrode Contacts in Final Fixture Design

As seen above the IPMC is placed between the two plastic fixture pieces. A compressive force is applied with a rubber band holding the IPMC in place and ensuring a good electrical connection. The spacing of the four solid core wires allows the IPMC electrodes to be activated individually while compensating for small changes in the electrode shapes.

FORCE AND DISPLACEMENT EXPERIMENTS

Using the new fixtures force and displacement experiments were performed to characterize the IPMC. This data will be used in the development of a finite element model as well as the closed loop control system. For the displacement experiments the IPMC was placed in its fixture below a CCD camera. The tip location was then identified using an edge tracking algorithm. The IPMC was given a step voltage ranging from .5 to

1.5 volts. This voltage was held constant throughout the bending process. Between each experiment the IPMC was placed back into deionized water for not less than five minutes.

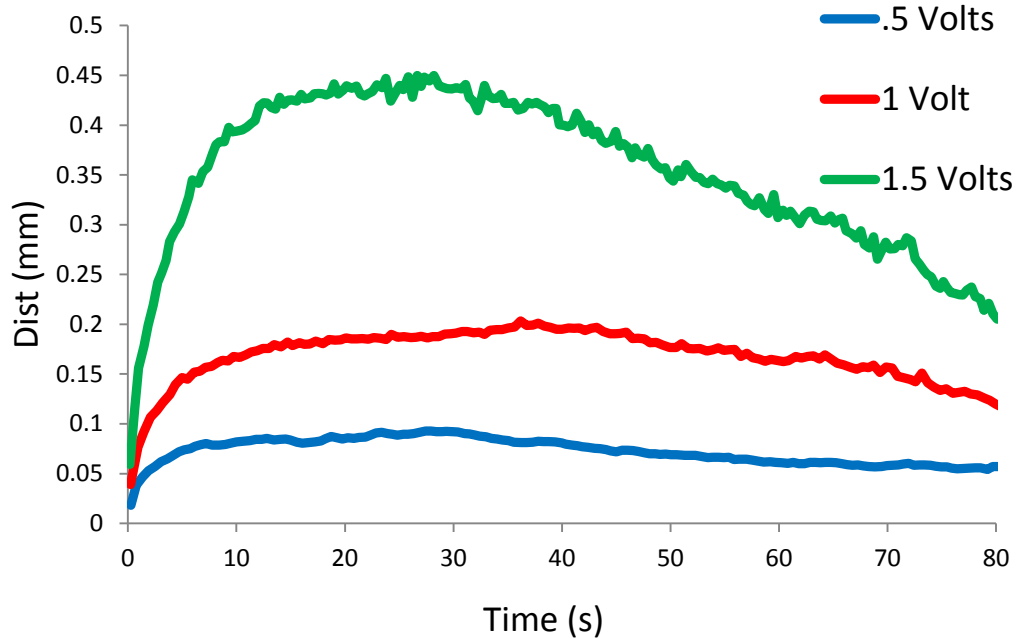


Figure 6 - Deflection Characterization of the Tube Type IPMC

As is common with most IPMCs, the tube type exhibits a quick initial bending towards the Anode [12]. After the initial bending the IPMC begins to slide backwards towards its initial starting position. This phenomenon is called relaxation and has been explained many ways [42]. The most widely accept hypothesis is that when activated the cations carry additional solvents and water towards the anode. After the initial motion these additional molecules begin to leak back out of this section causing the IPMC to relax its shape. Compared with flat type IPMCs of comparable length the tube type exhibits a much slower response and a much smaller maximum deflection [12]. This is

believed to be because of the added stiffness in the tube type IPMC shape, the smaller electrode surface area, and the overall size of the IPMC.

For the force experiments the IPMC tip location is not actively tracked. Instead force values are taken using a model 400a Force Transducer Sensor produced by Aurora Scientific Inc. This sensor has a full scale measurement range of +/- 50mN with a resolution of 1 μ N. This sensor utilizes a 1 mm in diameter boro-silicate glass tube as the force input device. The sensor is built to be actuated in the axial direction of the tube towards the sensor base. The sensor will still give a reading when actuated transversely however the accuracy of these values is much lower. As a result this glass tube was placed at the tip of the IPMC in the direction of bending. The tube was positioned to barely make contact with the IPMC. After the initial contact is made the sensor is adjusted to a new zero value. The IPMC is then actuated towards the sensor with voltage inputs ranging from .5 to 1.5 volts.

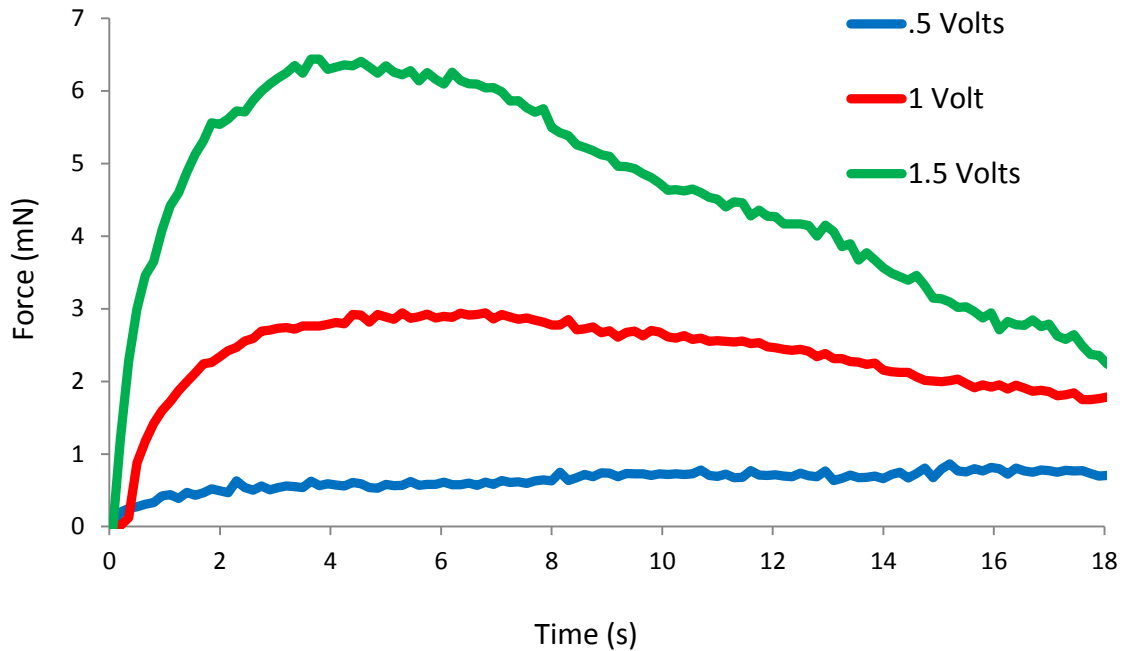


Figure 7 - Force Characterization of the Tube Type IPMC

As seen above the force and displacement results have very similar shapes. The maximum force produced by this tube type IPMC is 6.3 mN at 1.5 volts. This force value is much greater than the conventional flat type IPMCs when actuated at 1.5 volts [43]. This supports the belief that there is a tradeoff in IPMCs between the potential tip displacement and the force output. After the initial force peak the values continue to drop away. This is expected and is believed to be for the same reason that the IPMC position relaxes away. To further investigate the physical phenomenon seen within the tube type IPMC a multi-physics finite element model will be developed.

CHAPTER 3

FINITE ELEMENT METHOD

MATERIAL PROPERTIES, GEOMETRY, AND MESH

The multi-physics finite element model was developed using Comsol 4.3a. This tool is used to model the basic physics occurring within the IPMC. The models are developed to track the fluid interactions within the IPMC in the presence of an electrical field. These fluid interactions are then correlated to a mechanical bending force.

To produce this model the geometry of the IPMC will be idealized as a perfect circle with constant electrode shapes. These geometries were creating using the built in Comsol tools. Using the built in geometry tools allows the dimensions to be input as Comsol parameters and easily adjusted throughout the modeling process. To create the three dimensional a two dimensional IPMC cross section was drawn and then extruded to create the IPMC length.

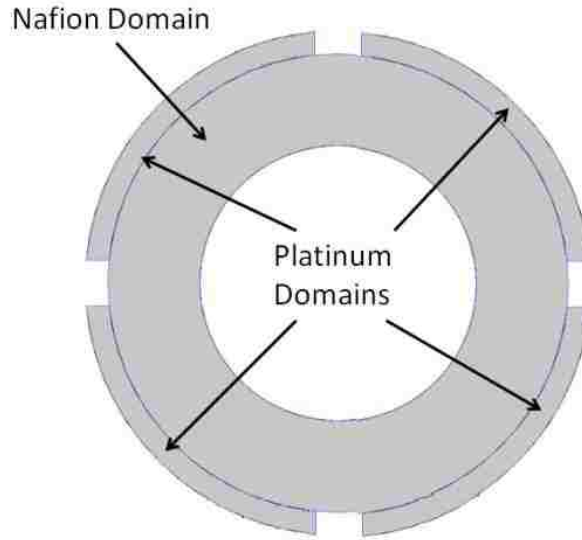


Figure 8 - IPMC Finite Element Model Geometry

In the center of the cross section is the tube shaped Nafion domain with the radii set to match the actual tube type IPMC samples. Surrounding the Nafion core are four platinum domains each separated by an isolation gap. Producing these isolated electrodes is quite difficult and the method for doing so has been discussed [44]. To produce these electrodes the platinum is not mechanically placed. It is instead chemically plated to the Nafion core and as a result the electrodes do not grow uniformly [19]. Improvements in the models accuracy can be achieved by modeling these growth patterns using fractals [18]. This increased accuracy comes at a cost of a much more computationally intensive model. In the Comsol model used these electrodes are presented as perfect geometries with a uniform contact surface between the Nafion and the platinum. As a result the electrical conductivity is greatly reduced in the multi-physics model to compensate for this simplification in geometry [45].

In the model the hole in the center of the IPMC is modeled as completely empty space. Although most IPMCs must be kept wet in order to function the movement of water molecules and the interaction with water molecules outside of the IPMC are not taken into account in this simulation. The simulation parameters can be seen in the table below.

Table 2 - Comsol Parameters and Variables

Parameters		
Name	Expression	Description
R	1.[mm]	Outer Radius
r	.95[mm]	Inner Radius
L	1[inch]	Extrusion Length
V1	1[V]	Voltage source
V2	1[V]	Voltage source
V3	0[V]	Ground
V4	0[V]	Ground
ro	.5[mm]	hole in the middle
Variables		
F	96458[C/mol]	Faraday Constant
eps	.2e-1[F/m]	dielectric permittivity
c_0	1200[mol/(m ³)]	Initial Concentration
D	.7e-11[m ² /s]	Diffusion Constant
eps_0	8.85e-12[F/m]	dielectric constant in vacuum
alpha	.001[N*m/mol]	Linear Force Coupling
beta	.0055[N*m ⁴ /(mol ²)]	Quadratic Force Coupling
mu	2.9e-15[mol*s/kg]	mobility

Table 3 - Comsol Material Properties

Platinum		
Name	Value	Unit
Density	21450	kg/m ³
Poisson's ratio	0.38	
Electrical conductivity	1.50E+04	S·m ⁻¹
Coefficient of thermal expansion	8.80E-06	1/K
Heat capacity at constant pressure	133	J/(kg*K)
Thermal conductivity	71.6	W/m*K
Relative permittivity	eps/eps_0	
Young's modulus	1.68E+11	Pa
Nafion		
Young's modulus	4.10E+07	Pa
Poisson's ratio	0.49	
Density	3105.5	kg/m ³
Electrical conductivity	5.00E+03	S·m ⁻¹
Relative permittivity	eps/eps_0	

MESH

The mesh was defined on the face of the IPMC and then extended along the length of the IPMC. This mesh has several features. It was designed to be fine near the Nafion platinum interface. This was accomplished using a distribution boundary condition. This condition guarantees that the number of elements in this critical region remains constant even when the hole size in the middle is varied. This region is considered critical because it is where the largest concentration changes are seen. Changing the mesh in these areas can lead to dramatic changes in the overall

concentration values. In contrast concentration changes in the longitudinal direction are quite small. The concentration changes in this direction do not contribute to the overall deformation changes. As a result the mesh in this direction was designed to be coarse. This mesh is seen as an acceptable compromise between accuracy and computational time.

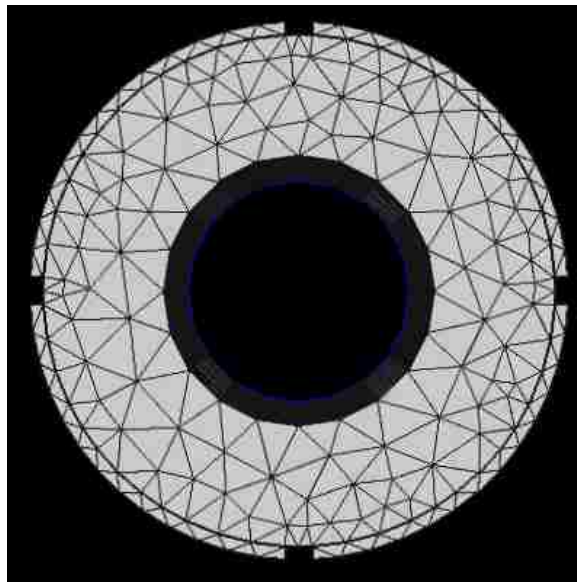


Figure 9 - Tube Type IPMC Finite Element Mesh

A more refined mesh could be used to more accurately model the concentration data near the electrodes. The model however breaks down when coupled with the deflection model when extremely fine meshes are used. These models could be decoupled and run independently however there would be an associated loss of accuracy.

MULTI-PHYSICS

To perform this simulation three physics packages were simultaneously used: electro-statics, transport of diluted species, and solid mechanics [45]. The electro statics analysis focuses on the input of the electrical field to the IPMC. This physics package is governed by the Poisson's equation:

$$-\nabla^2 V = \frac{\rho_s}{\epsilon} \quad 1$$

where V is the voltage, ρ_s is the space charge density, and ϵ is the dielectric permittivity. During the experiments only the section of the IPMC inside of the fixture is subjected to an outside voltage. To replicate this boundary condition in the simulation the tip of the IPMC is sectioned off. This smaller section is used to simulate the clamp boundary condition and as a result the electric potential is highest at the base of the IPMC.

With four electrodes there are many possible electrical inputs. The effects of different electrical inputs have been investigated in rod type IPMCs [24]. It has been found that the maximum displacement is achieved when 3 electrodes are activated with the remaining electrode acting as a ground. This configuration is easy to simulate but relatively difficult to achieve in an experimental setup. So instead for the initial simulations voltage will be applied to just one electrode and the electrode across the IPMC will be used as the ground. This replicates the most basic of deflection experimental setups.

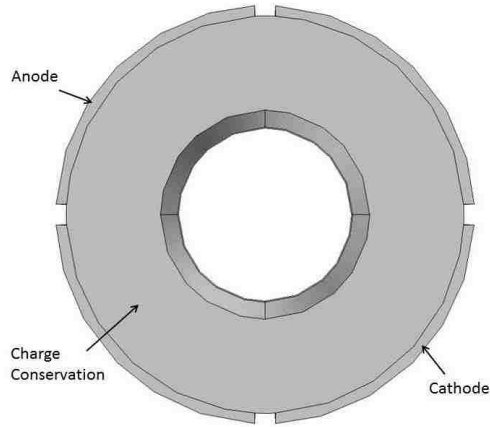


Figure 10 - Finite Element Electro-Statics Boundary Conditions

Initially the entire domain is set to a zero charge value. The one volt electric potential is applied as a step input at the beginning of the simulation. Using the electro statics model an electric field within the IPMC is calculated and sent on to the second physics package.

The second physics package used is the transport of diluted species. This package is used to describe the motion of charge particles due to the electric field and the fluid diffusion forces. The governing equation for this physics model is the Nernst-Planck plank equation:

$$\frac{\partial C}{\partial t} + \nabla \cdot (-D \cdot \nabla C - Z\mu FC \nabla V) = 0 \quad 2$$

where C is the cation concentration, D the diffusion constant, Z the particle charge number, μ the mobility, and F the Faraday constant.

Using this equation the induced cation concentration changes can be tracked within the polymer domain. With the anions rigidly attached to the polymer backbone this change in cation concentration causes a counter current to flow in the Nafion domain. It is this phenomenon that allows the IPMC to be used as both a sensor and an actuator. The transport of diluted species accepts the electric field as an input from the electrostatics model and sends back the counter current information. It is in this way that Comsol couples the multiple physics packages together.

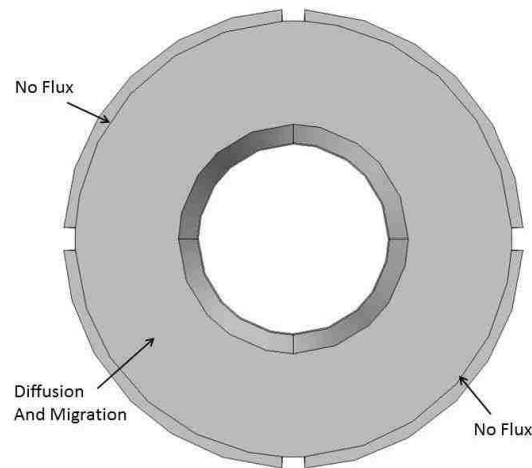


Figure 11 - Transport of Diluted Species Boundary Conditions

The transport of diluted species model is only used within the Nafion domain where the hydrated cations are allowed to flow freely [45]. As a result there are no flux boundary conditions between the Nafion and platinum domains. Electric current is still allowed to flow between the domains but no fluid particles.

The last physics packaged used in the simulation is the structural mechanics model. The bending in the tube type IPMC is being modeled using a linear elastic model:

$$\rho \frac{\partial^2 u}{\partial t^2} - \nabla \cdot \sigma = Fv \quad 3$$

where ρ is the density, u the deflection, σ the stress, and Fv is the volumetric body force. To use this linear elastic model the cation concentration change must be associated to a mechanical bending force. This relation has been modeled in several different ways. In this simulation the body force will be modeled as a polynomial fit of the space charge density [45].

$$Fv = \alpha \rho_s + \beta \rho_s^2 \quad 4$$

Where α and β are experimentally determined constants and ρ_s is the charge density.

The charge density in the IPMC is found using:

$$\rho_s = F(C - C_0) \quad 5$$

where F is Faradays constant, C the concentration, and C_0 the initial concentration [45].

The direction of bending is calculated automatically by examining the concentration gradients. In the bending model body force is only generated where there is a concentration gradient found. Since there is no fluid motion in the platinum these domains provide added rigidity to the simulation. As a result there is a tradeoff between adding additional platinum layers to improve the conductivity with the additional stiffness these extra layers will create [10].

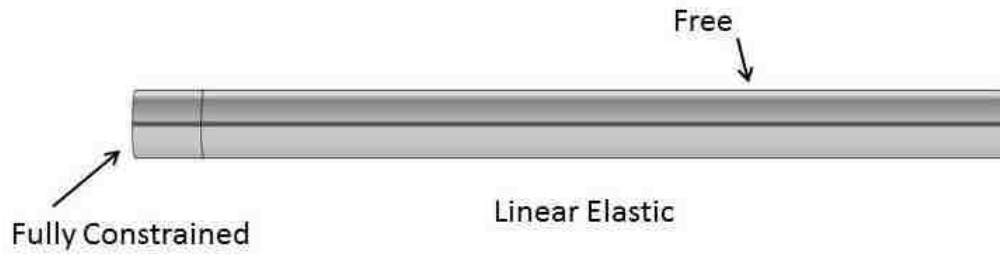


Figure 12 - Solid Mechanics Boundary Conditions

In the linear elastic model the base of the tube type IPMC is considered fixed in the X, Y, and Z directions. This represents the compressive effect of the clamp in the experimental setup. The rest of the IPMC is allowed to deform freely.

FINITE ELEMENT RESULTS

For the first simulation a 1 volt electric potential will be placed on a single electrode and a single ground will be used.

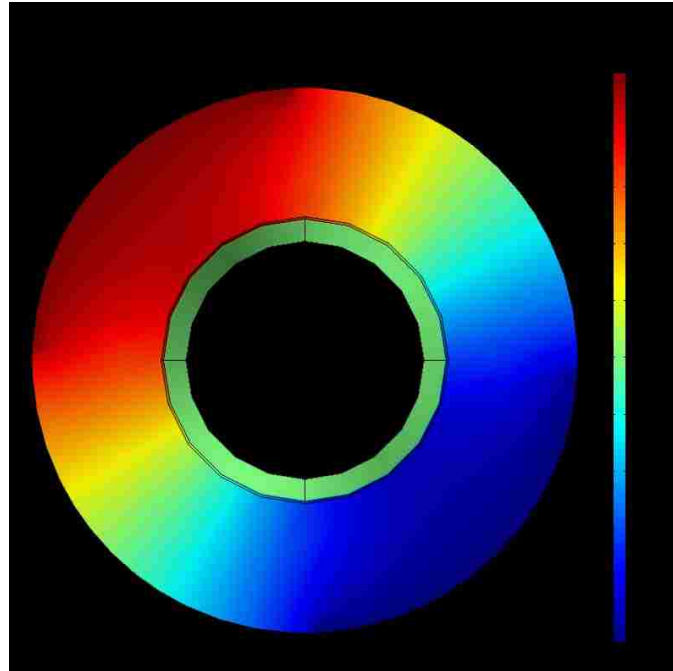


Figure 13 - Electro-Statics Results

The electric potential in the cross section of the IPMC can be seen in the figure above. Initially the entire domain was set to a zero charge. The electric field is seen spreading across the IPMC in a symmetric manner. Due to geometric inconsistencies in real samples this will not always be the case. As the simulation progresses the shape of the electric field changes and the potential drops near the electrodes become much more pronounced. This is believed to be a result of the counter current of the charged ions travelling across the IPMC. During the simulation these physics packages are coupled and the electric potential information is sent to the transport of diluted species model.

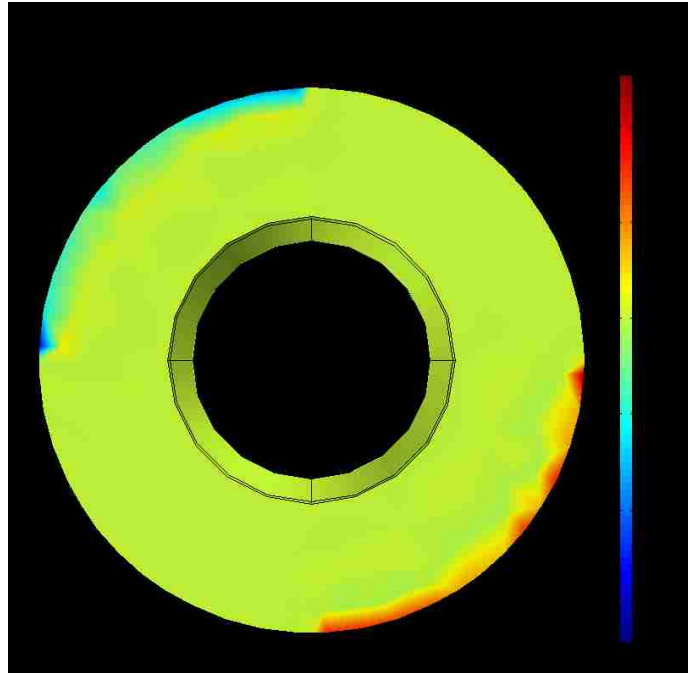


Figure 14 - Cation Concentration Levels

Initially there is a consistent 1200 mol/m^3 concentration value placed across the entire Nafion domain. With the addition of the electric field the particles begin to move and form a layer of charged cations near the cathode electrode leaving a void of cations near the anode. The width of this layer and the maximum concentration value can vary greatly depending upon the mesh used in the simulation. It is important during these simulations to check the mesh frequently and refine it when necessary. It is this change in concentration that causes the bending phenomenon seen in IPMCs. Water and other solvents within the IPMC would also be dragged across the Nafion domain however these particles are not considered in this analysis. The actual size of the charged particles is also not taken into account. There is a point where concentration values would be

unobtainable because of the relatively large size of the charge particles. In addition the growth of the platinum into the Nafion would impact the overall concentration levels. These potential issues will be discussed further in the future work section.

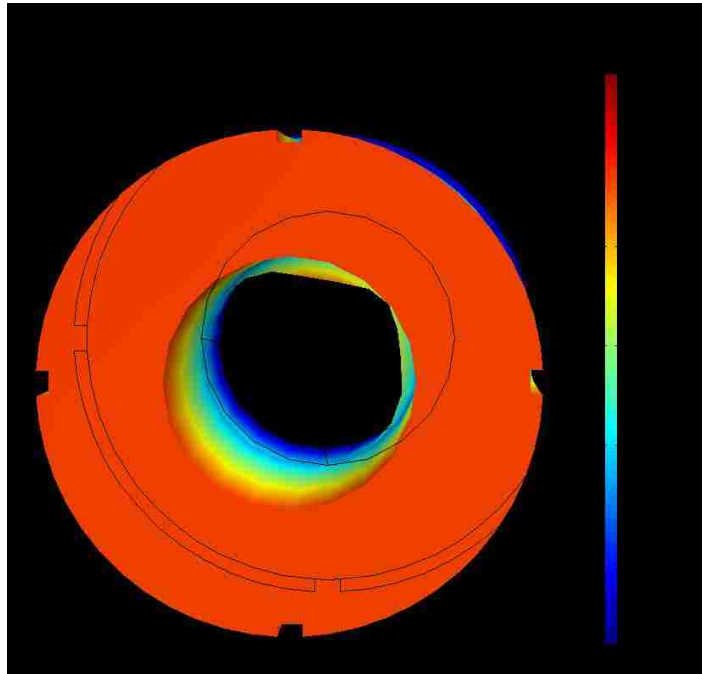


Figure 15 - Deformation of the Tube Type IPMC

For the first simulation the bending coefficients α and β will be set to .1 and .0055 [45]. The figure above shows the total tip displacement with a one volt input. The deformation occurs mainly in the section near the base where the change in electric potential is highest and therefore the change in concentration is highest. This is also seen in experimental setups where the majority of the bending happens at the base.

For the simulation a probe was placed at the tip of the IPMC to gather the total tip displacement during the simulation. This probe replicates the experimental practice of tracking the IPMC tip location and correlating this to the overall deflection. Using this displacement information the simulations can be compared against the experimental data.

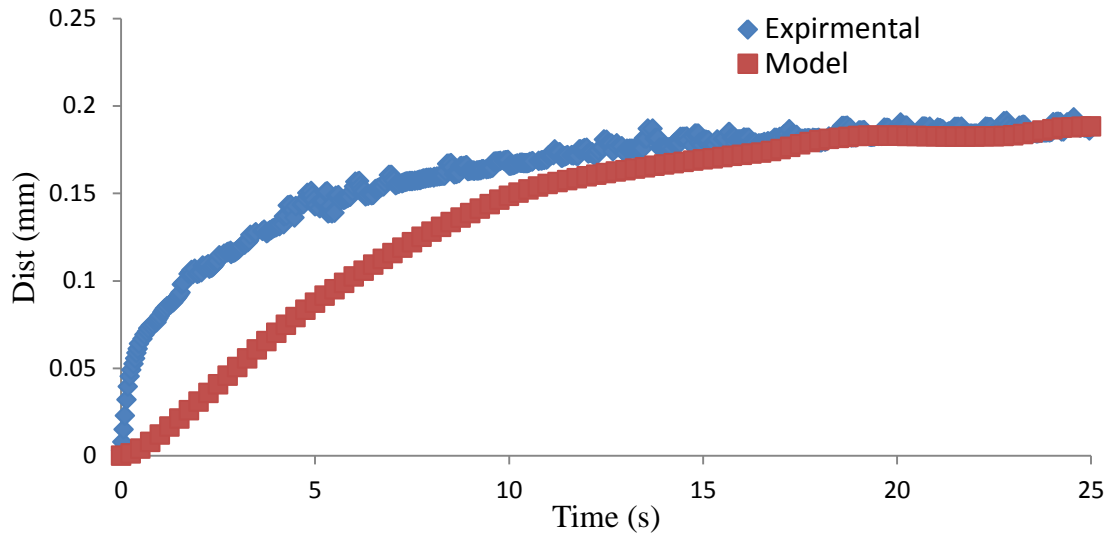


Figure 16 - Simulation versus Experimental Displacement

As seen in the figure above the Comsol simulation underestimates the initially bending seen in the IPMC, but the simulation eventually catches up to the experimental data and tracks pretty well. Some suggestions for model improvements have been to adjust the liner elastic model to achieve a faster initial bending force at the beginning.

With the calibrated model IPMCs can now be designed to meet specific size and displacement requirements. With previous flat type IPMCs the design options included, ionic polymer type, electrode material, electrode patterning, polymer thickness, electrode thickness, and overall width. All of these potential changes impact the IPMC form and function. With the tube type IPMC there are now two more design options, the hole size and ionic polymer thickness. The choice of these two parameters will also impact the overall IPMC function.

For the next simulation the effect of the hole size on the overall IPMC deformation will be investigated. With this simulation the IPMC diameter will be held constant and the size of the hole through the middle is varied. The outer diameter is set to 1 mm to match a rod type IPMC sample available at UNLV. The hole size will then be varied from 0 to .6 mm in diameter.

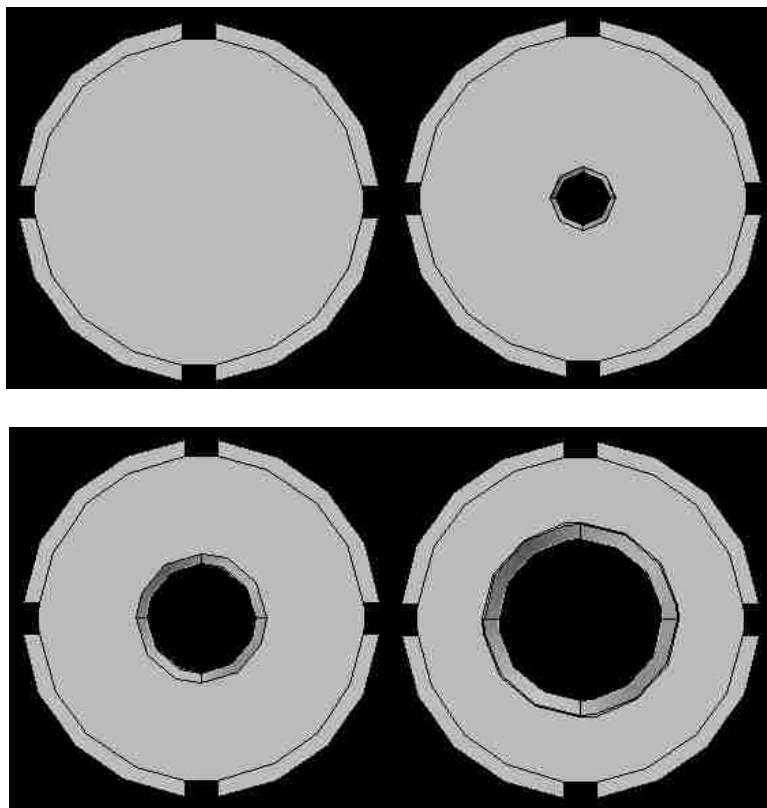


Figure 17 - Constant Diameter Varied Hole Diameter Simulation

For this simulation a 1 volt potential will be placed on a single electrode. The opposite electrode will be acting as ground. The simulation will be run for fifty seconds and the tip location for each sample will be tracked. The mesh around the hole will be refined for each new geometry, but the mesh near the electrode polymer interface will remain the same.

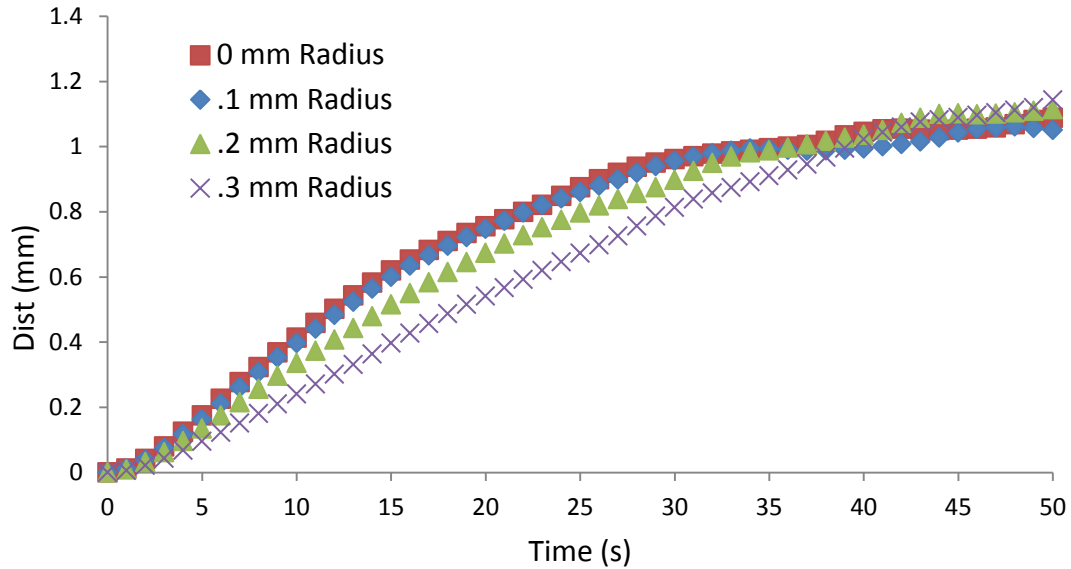


Figure 18 - Constant Radius Varied Hole Size Deflection Results

With the additional of a very small hole the bending characteristics of the IPMC are almost unchanged. The small hole does not significantly change the travel path of the cations and also does not have a large impact on the overall stiffness of the IPMC. As the hole grows in size and takes up proportionately more of the IPMC the deflection becomes significantly delayed. With the large tool holes the concentration gradients take longer to become established. By the end of the simulation the IPMCs with larger holes have deflected farther than the rod type IPMC. With a large hole through the middle the overall stiffness of the IPMC has been decreased.

In the previous simulation it has been shown that the hole size in the tube type IPMC can have a large influence in the overall bending performance. The bending performance is not the only design feature that needs to be taken into consideration. The

tool size desired also needs to be taken into account. For instance if the desired tool size is .6 mm in diameter at its largest point then the hole in the tube type IPMC would be sized accordingly. The bending motion of the IPMC can then be altered by changing the thickness of the nafion. To simulate this the hole radius will remain fixed while the Nafion radius is varied from .4 mm to .6 mm.

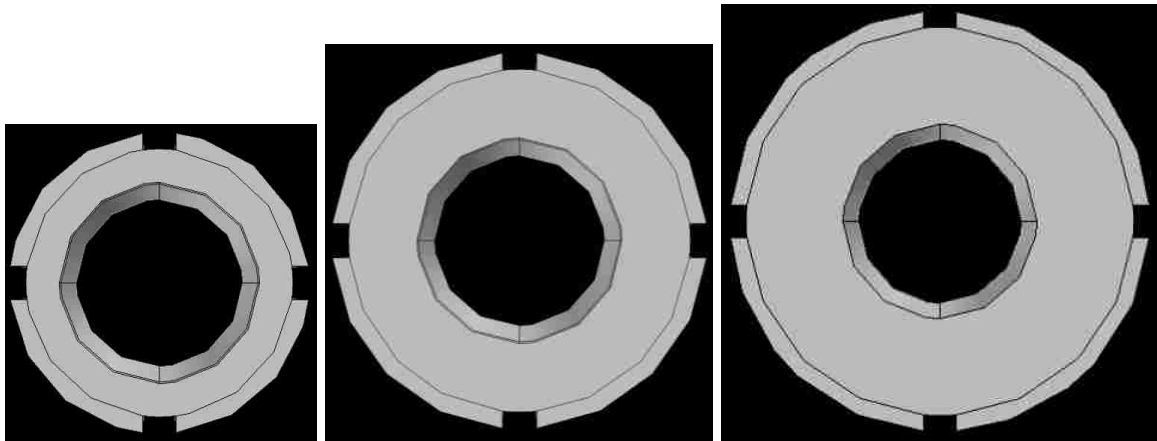


Figure 19 - Various IPMC Geometries

In this simulation the IPMCs are given a new electrical input with 1 volt placed along two electrodes with the other two electrodes operating as grounds.

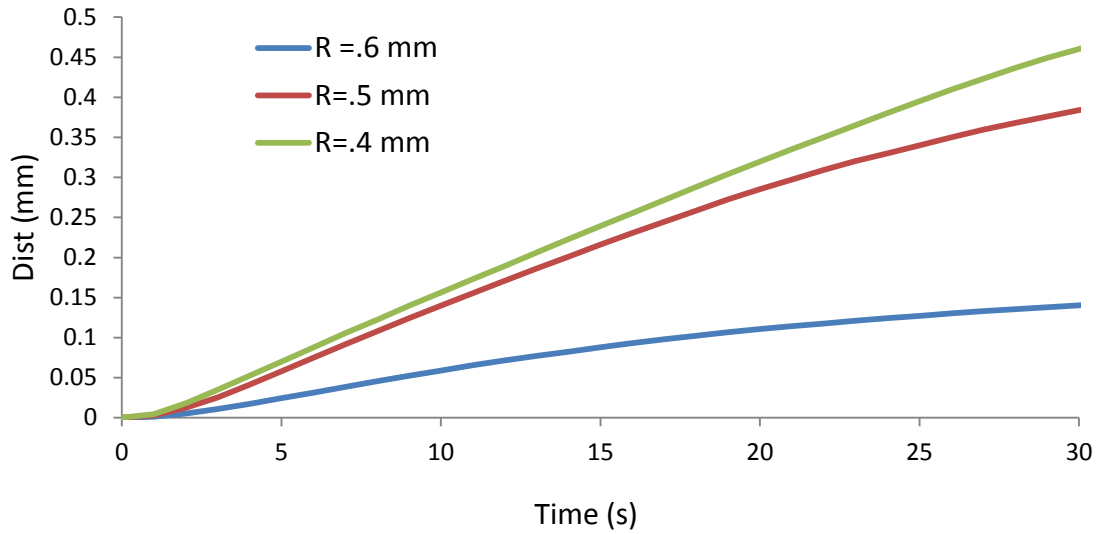


Figure 20 - Tube Type IPMC Deflection with Constant Hole Diameter

As the thickness of the Nafion layer gets smaller the total deflection found increases. This size IPMC would perform well in situations requiring a large deformation with low force applications. The finite element simulation allows the end user to determine the tube inner diameter to meet the desired tool size and then adjust the outer diameter to obtain the desired displacements. In both of these simulations the models were not able to be verified with experimental data. Further study with a wider variety of tube type IPMCs will have to be conducted to verify the simulated results.

CHAPTER 4

CLOSED LOOP CONTROL

ELECTRO-MECHANICAL MODELING

In the previous section a finite element model for designing and customizing tube type cylindrical IPMCs was presented. With this model in hand IPMCs can be made to fit specific tasks in specialized industries. To utilize these new IPMCs a method for controlling the tip location is developed. This is accomplished using an electro-mechanical model of the tube type IPMC. As seen in previous research the electrical properties of an IPMC can be modeled with a lumped RC model [17]. The IPMC is described as having a double-layer capacitor created in the boundary between the metal electrodes and the ionic polymer.

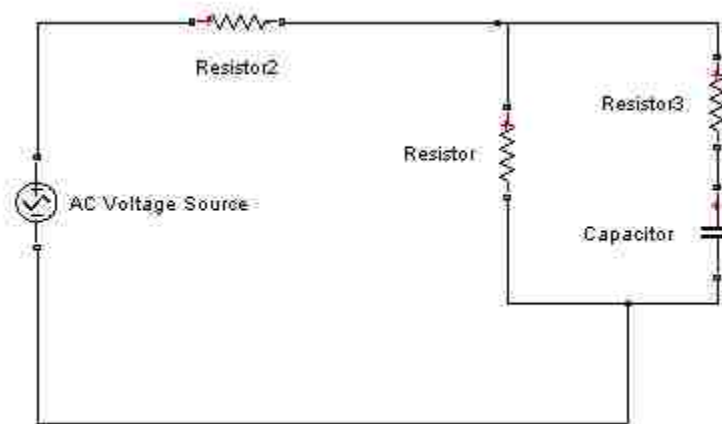


Figure 21 - RC Circuit Model

The RC model is verified by performing several electrical tests on the tube type IPMC. For the first test a step voltage was applied across the tube type IPMC and the voltage and current responses were measured.

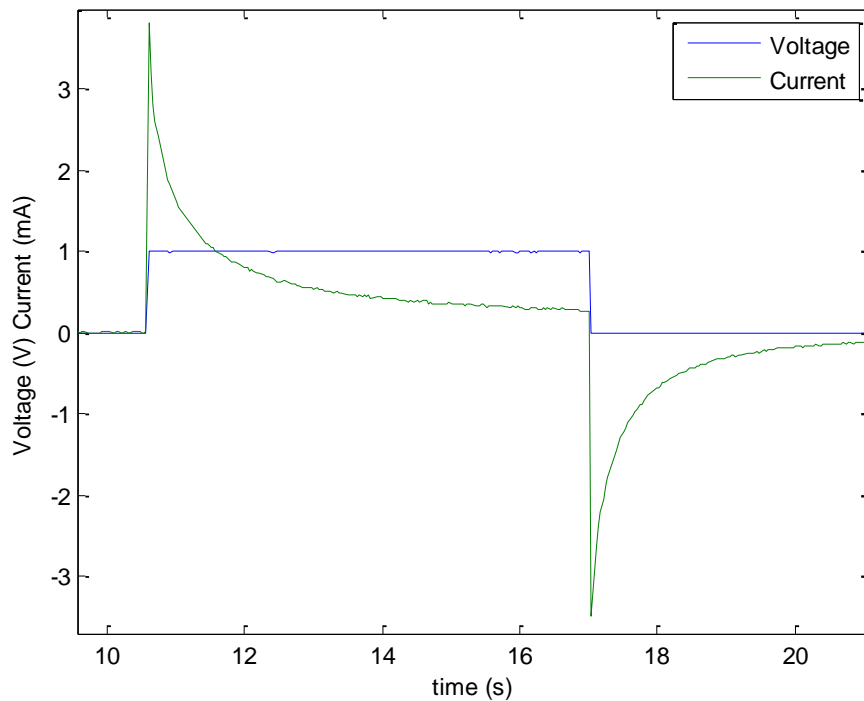


Figure 22 - Electrical Step Response of IPMC

As seen above the current does not return to zero after the step voltage input. If the circuit was purely capacitive then the current should have eventually returned to zero. Since it instead has a steady state value there must be a resistor in the electrical model. The resistance value can be calculated using the steady state current and voltage values.

For the second electrical test a sinusoidal signal was applied to the IPMC with a peak voltage of 2.5 volts. As seen the voltage and current are out of phase with one another. In this test the current is leading the voltage which denotes a capacitive circuit. If this were a purely capacitive circuit the phase difference would be 90 degrees however this is not the case. To model this effect a resistor is placed in series with the capacitor leading to the clumped RC circuit model.

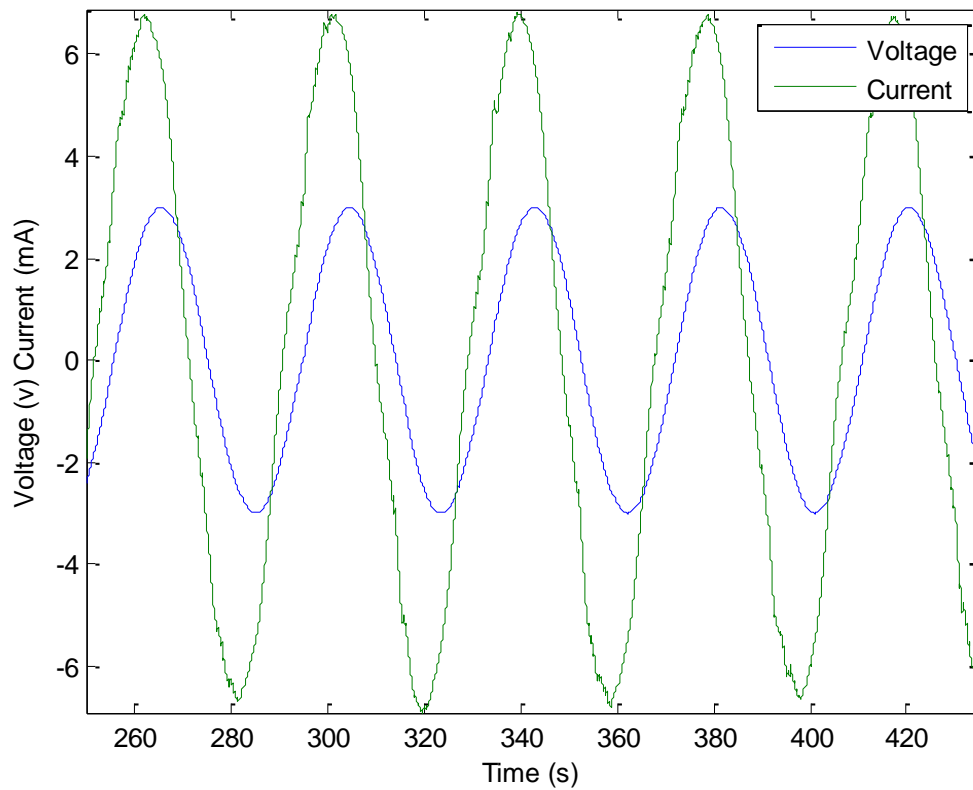


Figure 23 - Sinusoidal Voltage Input IPMC

Using this data the capacitance of the IPMC can be calculated. The complex impedance was calculated using a curve fit of the sinusoidal data. Using this curve fit the complex voltage and complex current was calculated. The curve fit was accomplished using a Matlab curve fitting algorithm at varies input frequencies.

$$V = |V|e^{j(\omega t + \phi v)} \quad 6$$

$$I = |I|e^{j(\omega t + \phi I)} \quad 7$$

$$Z = |Z|e^{jarg(Z)} \quad 8$$

The complex impedance can be further split into a real and imaginary part. The imaginary part called the reactance is only influenced by an inductance or a capacitance in the circuit. In the RC model there is no inductance so the capacitance can be calculated from the reactance data. The capacitance of the tube type IPMC was found to be .15 mF which is within the range of expected values for an IPMC [6] .With these experimental values the electrical effects of our IPMC circuit can be simulated.

Using this circuit model the charge within the IPMC is studied. The movement of charge within the IPMC can be modeled using the standard ODE for an RC circuit.

$$R \frac{dq}{dt} = V - \frac{q}{C} \quad 9$$

where R is the resistance, q the charge, V the voltage, and C the capacitance. This equation can be solved under a step voltage input which yields:

$$q = VC \left(1 - e^{-\frac{t}{RC}}\right) \quad 10$$

To complete the electromechanical model the electrical model is correlated to the macroscopic bending motion. Several methods for modeling the IPMC have been discussed [22]. Many of these methods rely upon splitting the IPMC along the length into several finite element lengths [1]. This method gets more accurate by increasing the number of finite elements used. To effectively use this method multiple points along the IPMC length are tracked. Most experiments accomplish this by positioning a camera out of the plane of motion and tracking several markers. As a result this method is mostly commonly used for a single bending motion [1]. With a biaxial bending IPMC tracking multiple points in both bending directions along the side of the IPMC is impractical. As a result the curvature of the IPMC will be related to the moving charges instead of the overall deformation [18]. The curvature model was first used without a time constant to describe the back relaxation and although the IPMC does not deform into a perfect arc this is believed to be a reasonable approximation to the deformed state.

$$\frac{dk}{dt} = \frac{1}{\tau}(cV - k) \quad 11$$

Where k is the curvature, V is the voltage, c the saturation curvature at a unit applied voltage, and τ the time constant [18]. This equation matches the initial bending well is unable to compensate for the relaxation seen in several different types of IPMCs. To describe this phenomenon a more general equation is used.

$$\frac{dk}{dt} = K_1 \frac{dq}{dt} - \frac{1}{\tau_2}(k - K_2q) \quad 12$$

Where q is the electric charge, K_1 the coefficient of bending during the initial bending phase, K_2 the coefficient of bending during the equilibrium state, and τ_2 is the relaxation time constant [18]. This model is capable of following the IPMC tip through the initial deflection and slow back relaxation. This ability was not replicated in the previous multi-physics finite element model which did not include the motion of water or other solvent particles.

Combining this equation with the previous RC circuit model yields an equation that relates the curvature of IPMC k to the input voltage V over time t .

$$k = V \left(\frac{K_{v2}\tau_1 - K_{v1}\tau_2}{\tau_2 - \tau_1} e^{-t/\tau_1} + \frac{\tau_2(K_{v1} - K_{v2})}{\tau_2 - \tau_1} e^{-t/\tau_2} + K_{v2} \right) \quad 13$$

where $K_{v1} = CK_1$ and $K_{v2} = CK_2$ [18]. Although this equation specifies the curvature of the IPMC this is a difficult value to determine experimentally. Instead this curvature value will be related to the tip displacement δ .

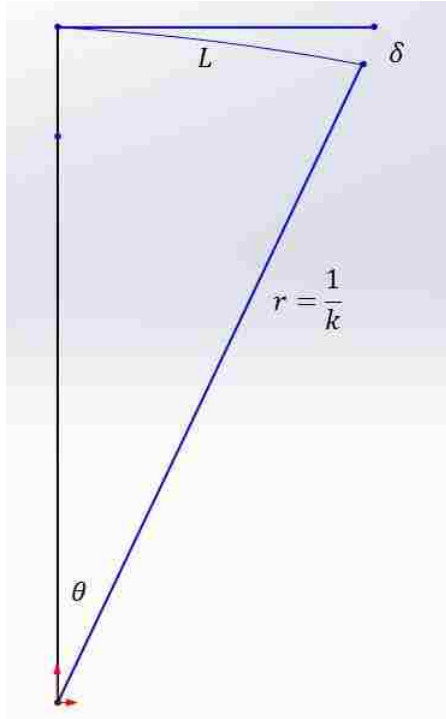


Figure 24 - Curvature to Displacement Conversion [25]

Using some basic geometry the tip displacement can be found [25].

$$\delta = r(1 - \cos\theta) = r \left(1 - \cos\left(\frac{L}{r}\right) \right) \quad 14$$

Taking the Taylor series expansion of cosine and approximating to the second order terms leads to:

$$\delta \approx \left(1 - \left(1 - \frac{1}{2!} \left(\frac{L}{r}\right)^2 \dots \right) \right) = \frac{L^2}{2r} = \frac{L^2}{2} k \quad 15$$

Taking this result and relating it to the previous bending equation yields:

$$\delta = \frac{VL^2}{2} \left(\frac{K_{v2}\tau_1 - K_{v1}\tau_2}{\tau_2 - \tau_1} e^{-t/\tau_1} + \frac{\tau_2(K_{v1} - K_{v2})}{\tau_2 - \tau_1} e^{-t/\tau_2} + K_{v2} \right) \quad 16$$

This equation relates the simple tip deflection to the input voltage to the IPMC base. This bending equation is now applied to two bending directions and two input voltages. The coefficients for these equations are also lumped together for simplicity [25].

$$X = \frac{V_X L^2}{2} (A_X e^{-a_X t} + B_X e^{-b_X t} + C_X) \quad 17$$

$$Y = \frac{V_Y L^2}{2} (A_Y e^{-a_Y t} + B_Y e^{-b_Y t} + C_Y) \quad 18$$

To calibrate these equations the coefficients must first be calculated. This is accomplished by curve fitting these equations to the basic IPMC displacement experiments performed earlier.

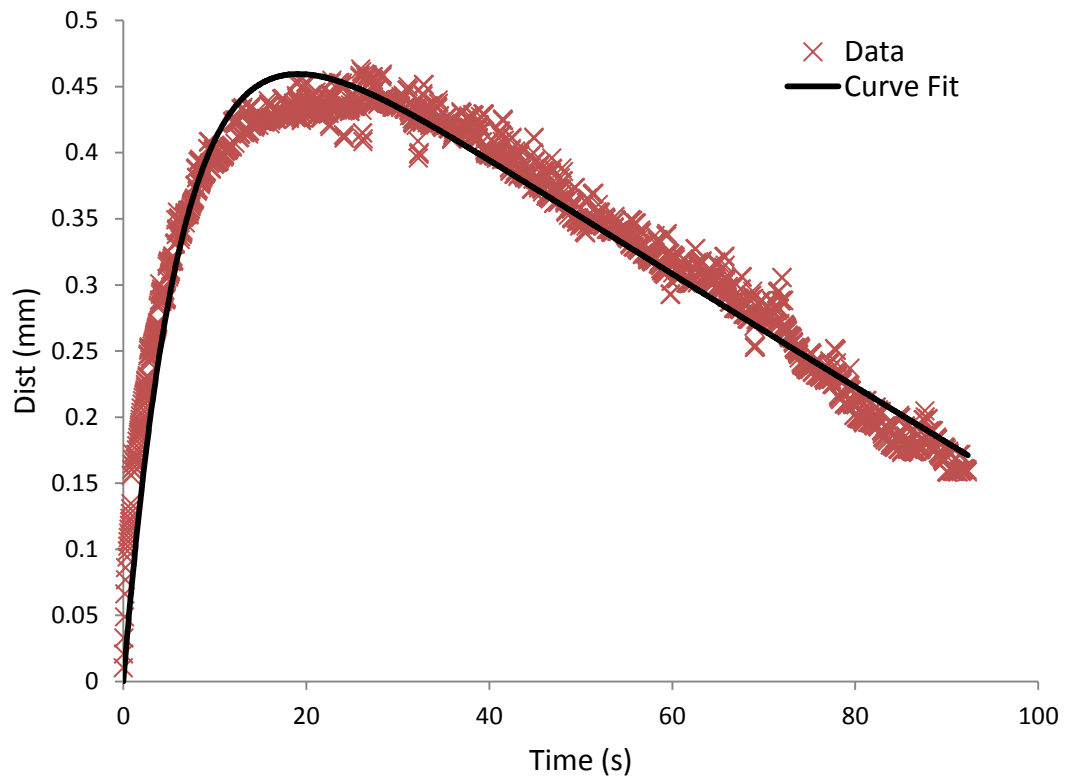


Figure 25 - Deflection Curve Fit at 1.5 Volts

As a result of the different sizes between the IPMC samples and the uncertainties in the IPMC manufacturing process the calibration process must be repeated for each individual sample and bending direction. It is also a good practice to re-calibrate the models as time progresses to compensate for the changes in the IPMC bending characteristics.

Table 4 - Curve Fit Coefficients

Name	Value
L	23.18
Ax	0.018333
ax	0.000925
Bx	-0.00214
bx	0.157272
Cx	-0.0162

CONTROLLER DESIGN

Now that a full electromechanical model has been developed the transfer function of this model is derived. The outputs of the model are the X and Y deflections. The input of the model will be set as a step voltage input for the first simulations. First the Laplace transform of the displacement equations is taken [25].

$$X(s) = \frac{L^2}{2} \left(\frac{A_x}{s + a_x} + \frac{B_x}{s + b_x} + \frac{C_x}{s} \right) \quad 19$$

$$Y(s) = \frac{L^2}{2} \left(\frac{A_y}{s + a_y} + \frac{B_y}{s + b_y} + \frac{C_y}{s} \right) \quad 20$$

Secondly the Laplace transform of the step input voltages are taken.

$$U_x(s) = \frac{V_x}{s} \quad 21$$

$$U_y(s) = \frac{V_y}{s} \quad 22$$

Combining these equations yields the open-loop transfer functions for the IPMC deflection under a step input [25].

$$T_x(s) = \frac{L^2 (A_X + B_X + C_X)s^2 + (A_X b_X + B_X a_X + C_X(a_X + b_X))s + C_X a_X b_X}{2 V_X(s^2 + (a_X + b_X)s + a_X b_X)} \quad 23$$

$$T_Y(s) = \frac{L^2 (A_Y + B_Y + C_Y)s^2 + (A_Y b_Y + B_Y a_Y + C_Y(a_Y + b_Y))s + C_Y a_Y b_Y}{2 V_Y(s^2 + (a_Y + b_Y)s + a_Y b_Y)} \quad 24$$

The first test performed was to simulate the open loop response of a 1 volt step input along the x axis. This simulation is performed to validate the transfer function's accuracy and ensure that no modeling errors have occurred.

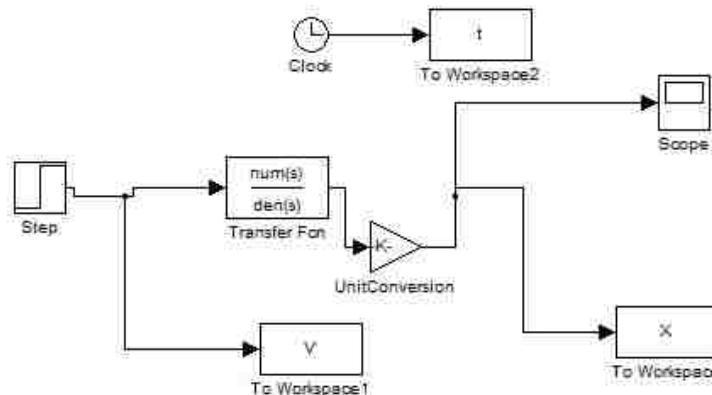


Figure 26 - Open Loop Simulation Schematic in Matlab Simulink

For the simulation two control systems are proposed and advantages of each are discussed. The first control system is a standard PI controller. The experimental setup uses an edge detection algorithm to locate the IPMC tip. This method produces a jumpy

signal that causes quickly changing position data. With the inaccuracy in the experimental location of the IPMC tip it was decided to not implement a derivative controller. The controller was implemented in the Simulink environment and tested with several transfer function coefficients representing the various tube type IPMC samples.

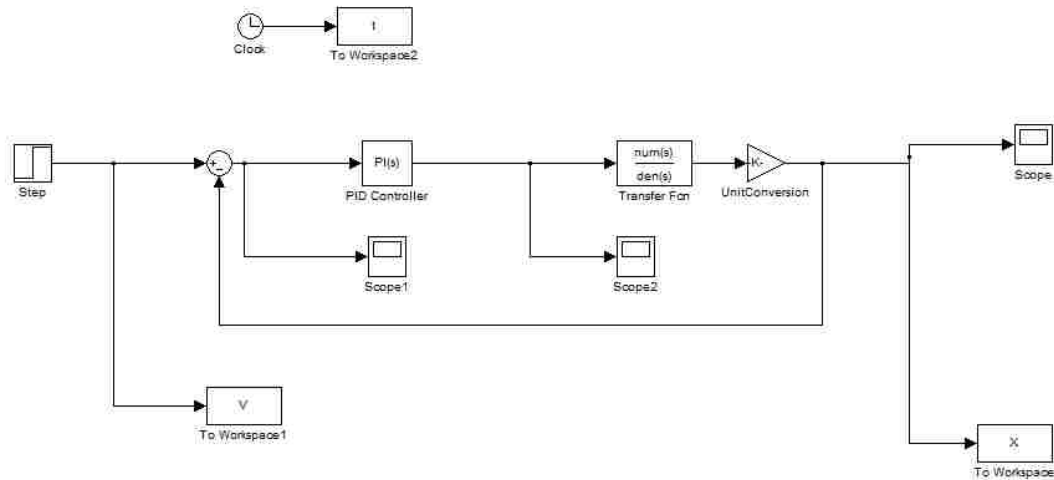


Figure 27 - Closed Loop PI Controller

The proportional and integrative gains were tuned to provide a fast response and limit the long term errors in the models. The proportional gain K_p was set to 34 and the K_i gain was set to 93 for this simulation the position and error are reported in mm. For this initial simulation the IPMC will be asked to hold a X position of .3 mm.

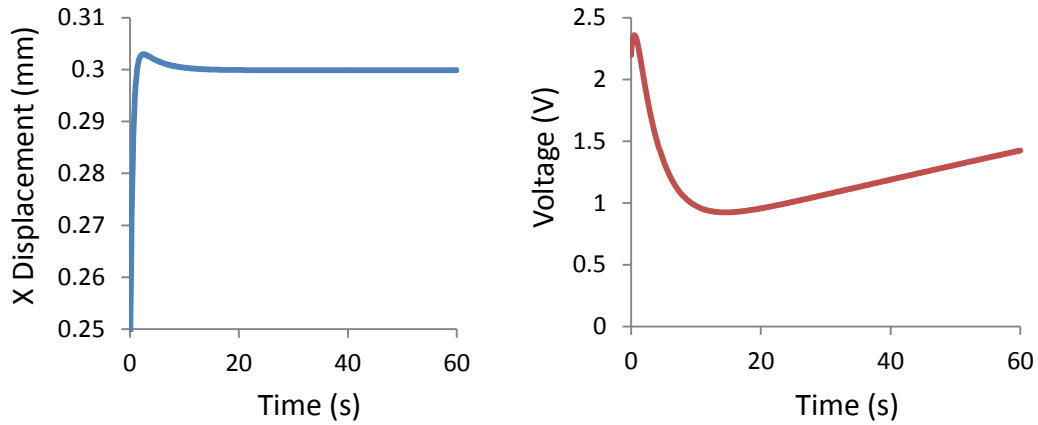


Figure 28 - Deflection and Voltage Simulation Data

The error tracking performance of the system is quite good. There is a small overshoot of the desired trajectory but the time response acquires the desired value within a few seconds. In order to provide this fast response the voltages seen are initially quite high. The high voltage levels could be potentially dangerous to the IPMC so saturation levels will have to be implemented during the experimental trials. After the initial peak the voltage stabilizes and begins to rise again to counteract the relaxation of the tube type IPMC.

The second control law can be expressed by the following equation:

$$V = V_{ss} + K_p e + K_i \int e dt \quad 25$$

Where V_{ss} is the steady state voltage, e the error, K_p the proportional gain, and K_i the integral gain. This control law relates the maximum tip displacement to a steady state voltage needed to achieve this deflection. The displacement results for voltages ranging

from .5 to 2.5 volts were plotted and a curve fit relating the input voltage to the maximum displacement was calculated.

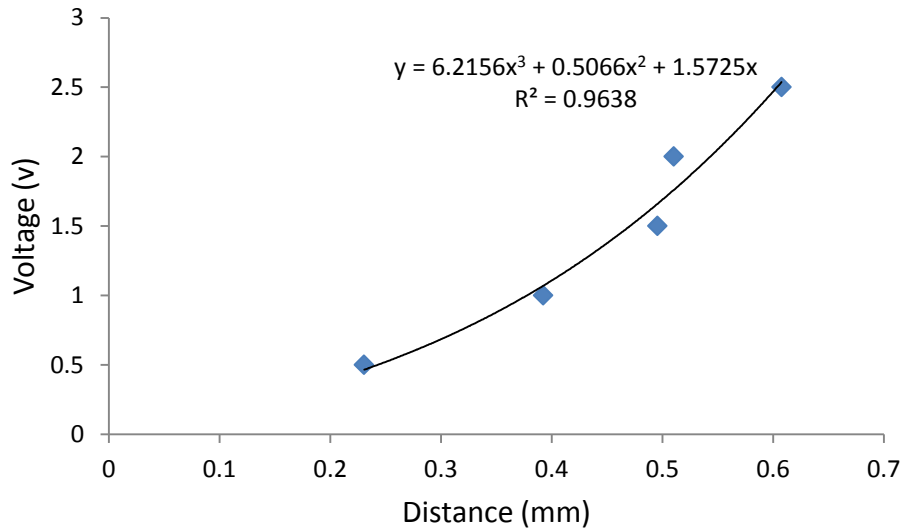


Figure 29 - Maximum Displacement Correlated to Voltage

The desired location is taken and translated into a steady state voltage signal needed to obtain that distance. This new control law is then simulated using the same tests in Matlab Simulink

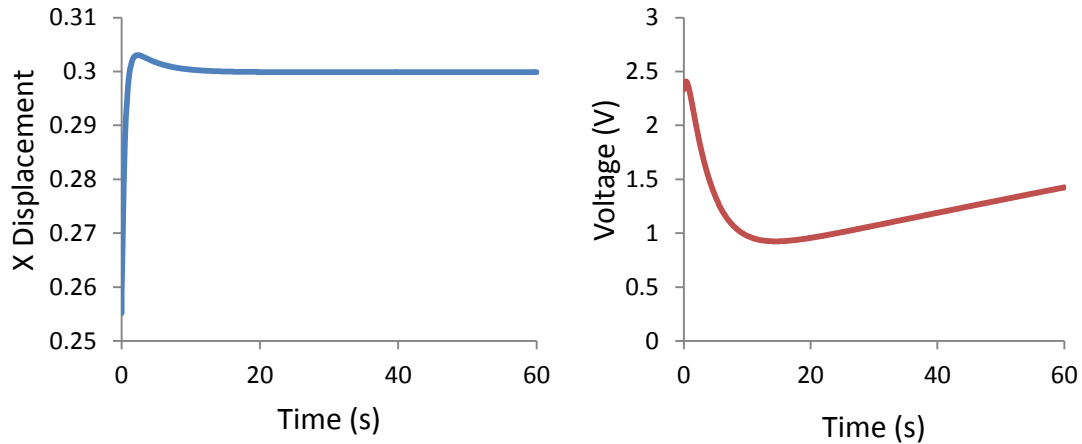


Figure 30 - Control Law Simulation for Steady State Voltage

As shown in the figure above the performance of the two control laws is nearly identical. The plotted steady state voltage makes very little difference in the actual performance of the system. The given steady state value gets easily overrun by the PI controller values. There is also a computational cost for implementing this more complex system. The curve for calculating the needed voltage values would also have to be extended to negative desired deflection values. This would further expand the computational resources needed to implement this control law. As a result the more simplistic first control law will be used.

The control law chosen is extended to two desired trajectories X and Y position. This simulation will be used to track a circular trajectory with IPMC tip. This trajectory will then be experimentally studied and the results will be compared. While running these simulations the voltages used will be carefully studied. With the actual IPMC large voltages can cause electrolysis within the sample and potentially damage the polymer

itself. As a result the voltage has been limited in the experimental setups to 1.5 volts. This restriction will be replicated in the simulations by saturating the voltage output of the PI control law at 1.5 volts.

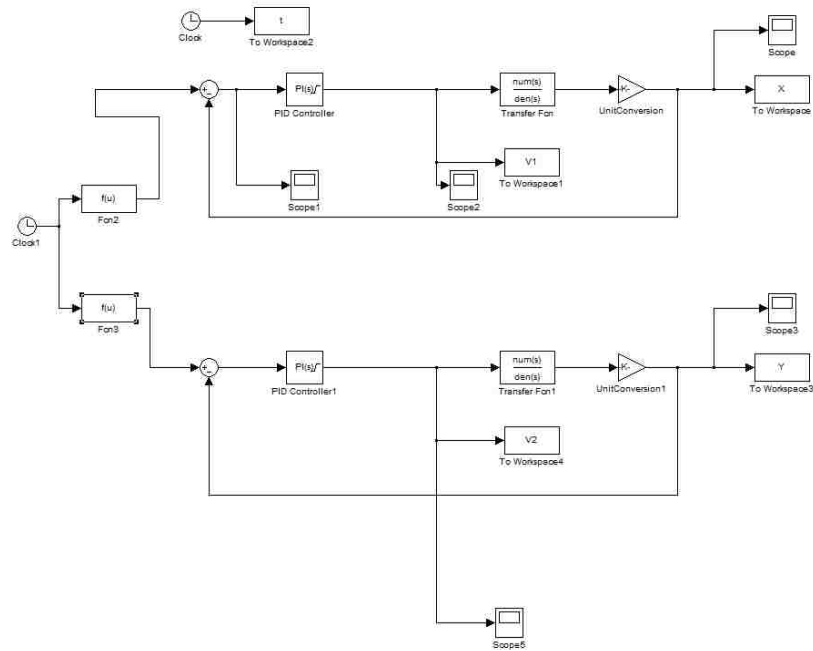


Figure 31 - Circular Simulation with 1.5 Volt Saturation

Above is the Matlab Simulink used to simulate the circular trajectory and IPMC tip following. The time constant for the circle trajectory is varied to match the experimental setup as best as possible. The direction of rotation has also been adjusted to match the experimental data. The radius of the circle has been set at .2 mm. With this radius the only point at which the voltage saturation should occur will be on the initial

push to move the IPMC from the origin to the circular trajectory. With the inconsistencies in the actual IPMC samples it will be a better test if the radius is kept within easy reach of the IPMC at the given voltage saturation levels.

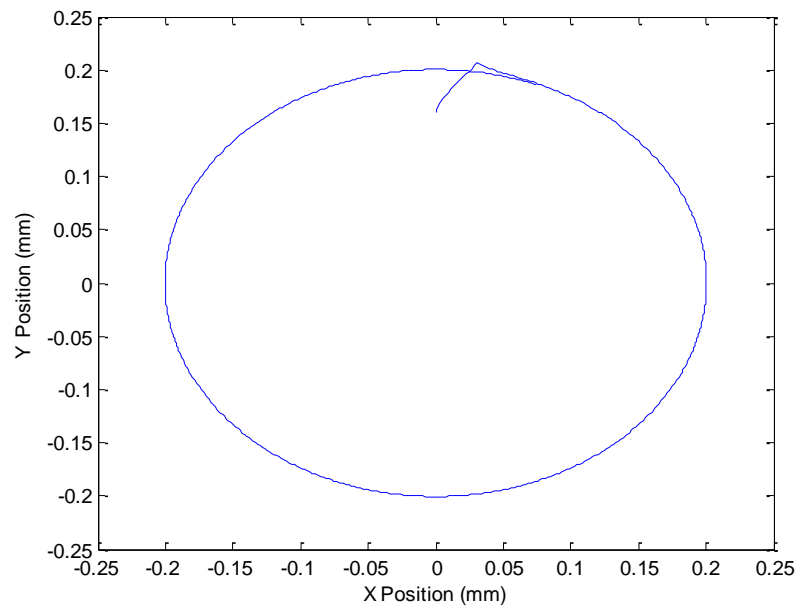


Figure 32 - Simulation of circular trajectory following

As seen above the IPMC simulation follows the circular trajectory quite well. There is a slight overshoot as expected from the previous simulations. The maximum displacement of the IPMC at 1.5 volts is actually greater than .2 mm so the overshoot is still occurring. The voltage saturation also allows a greater level of error to build up in the simulation then when no saturation is used. This error causes the sharp corner seen in

the above simulation. This simulation result will be compared against real world data in a later section.

EXPERIMENTAL SETUP

With the simulation results in hand the proposed control laws were implemented in an experimental closed loop setup. The experimental setup includes a Labview PXI 1042Q box where an edge tracing algorithm is used to locate the IPMC tip location. This data is then fed into the PI controller which produces two sets of control voltages. The voltages are sent through a pin box to two HA-151 Potentiostat/Galvanostats connected to the IPMC. An image of the IPCM is then captured by an STC-630 CCD camera and fed back into the Labview VI.

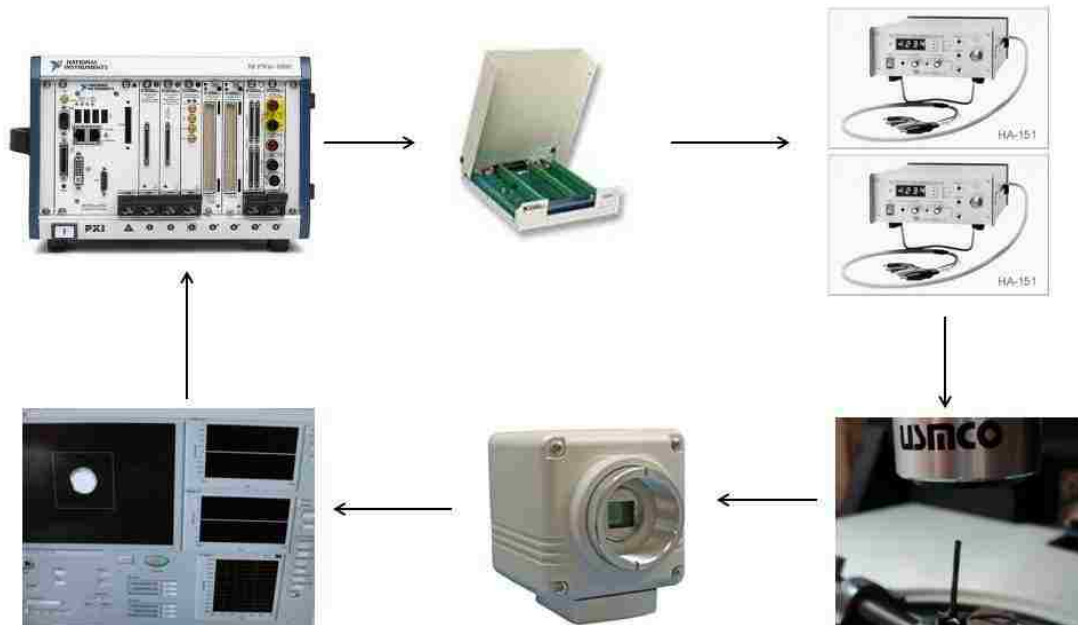


Figure 33 - Closed Loop Control Experimental Setup

The Labview PXI bus has several interchangeable slots allowing this device to be customized to many applications. The bus has an on-board NI PXI-8196 embedded computer running Windows 7. For these experiments the NI PXI-1411 Image acquisition and NI PXI-7833R Reconfigurable I/O modules are used. The PXI-1411 module has a BNC connector for the video source capable of 30 frames/s of video in NTSC format. The PXI-7833R module has 8 configurable analog output channels with a voltage range of +/- 10 volts. The module also has 8 configurable analog input channels with an input range of +/- 10 volts. This module is also a field programmable gate array (FPGA) allowing for basic calculations to be performed on the module itself. Once the desired output voltages are calculated the PXI box sends two control voltages through the pin box to the two potentiostats.

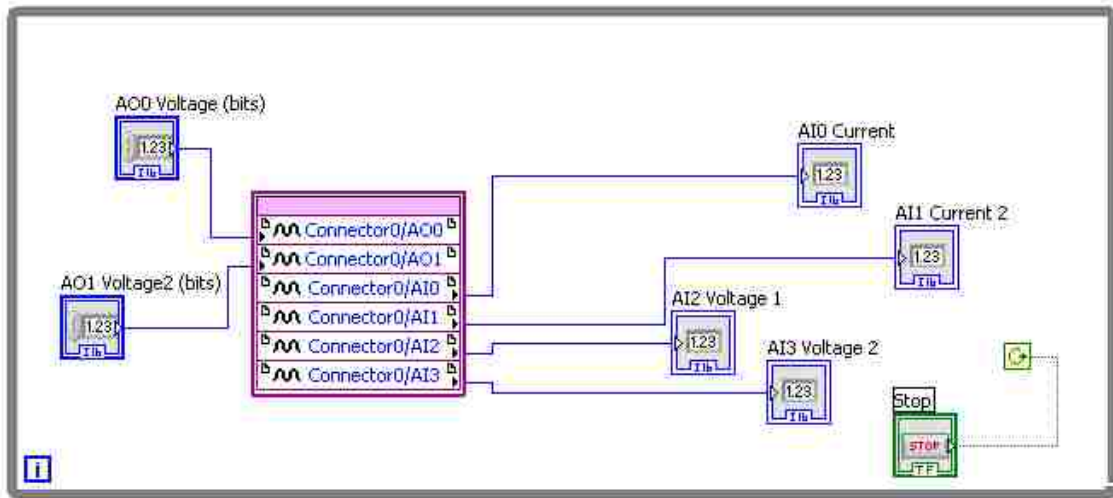


Figure 34 - Labview PXI-7833R FPGA Assignment

The Potentiostats are each attached to the IPMC. There is one Potentiostat controlling the X voltage and the other controlling the Y voltage. Both boxes are operated in Potentiostats mode with the external control on. These boxes receive the control voltage signal before amplifying it and sending the voltage to IPMC. The boxes then record the voltage and current found across the IPMC and send these signals back to the Labview PXI box.

The IPMC is secured in a clamped fixture which is placed on a micromanipulator table. The micromanipulator has a built in microscope and the ability to control the motion of the table and the microscope. This allows for easy focusing and centering of the IPMC tip in the image field. The microscope provides a ten times image magnification and is equipped with a CCD camera sending a live feed back to the Labview PXI box. To calibrate this camera a grid with known spacing was placed

beneath the microscope. The spacing was tested to find the conversion factor between pixels and mm. It was found that there are 108 pixels per mm with very little image distortion along the edges.

In order to accurately locate the IPMC tip an edge detection algorithm is programmed into the Labview PXI box. To get a more stable signal a white marker is placed on the tip of the IPMC and the background is blacked out to provide the greatest contrast possible. The camera then captures this image and sends the file back to the Labview PXI box. The signal comes in as a 644X482 32 bit RGB image file at 30 frames per second. Color images are much more difficult to detect contours in so a single color pane is extracted. This color pane is a selectable parameter and is chosen to provide the greatest image clarity. By extracting a single pane the signal is reduced to an 8 bit image file.

This file is then sent to a contour extraction algorithm. The algorithm looks for a change in pixel values over a user defined threshold. This value is set as high as possible without causing the algorithm to lose the contour. The higher the threshold value is the less noise is seen on the signal. The search is conducted through the region of interest (ROI) searching for the longest continuous contour. When found the algorithm sends the x and y coordinates of every point in the contour on to the next step. The next block takes the contour points and creates a best fit circle to match the data. The center point of this circle is then taken to be the tip location of the IPMC.

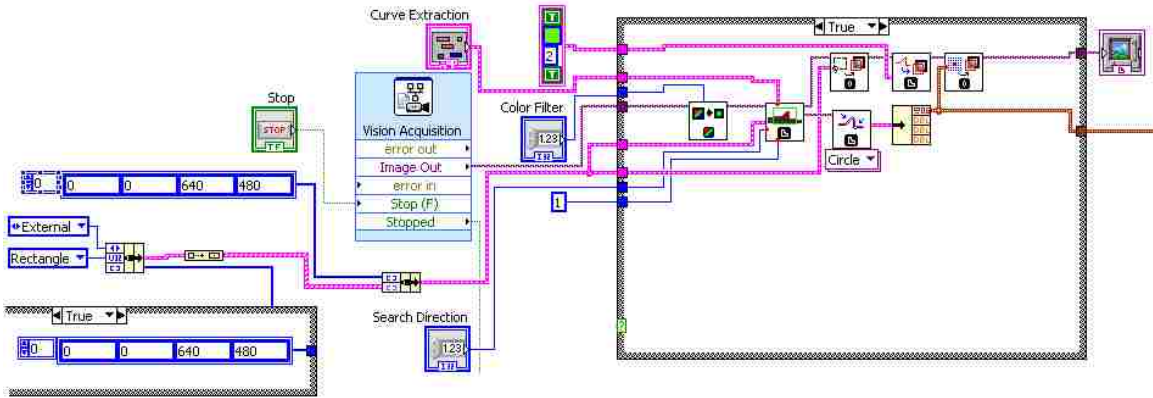


Figure 35 - Labview Contour Extraction VI

In order to minimize the computer resources used the contour tracking algorithm does not search the entire screen every time. For the first iteration the entire screen is used to locate the largest possible contour. The center point of the best fit circle is then calculated. Using this position a new ROI is calculated centering on the previous center point. With the relatively slow bending speed of the IPMC compared to the image acquisition rate this ROI can be made quite small. By cutting down on the search area the overall computational resources used to perform this image tracking are greatly reduced.

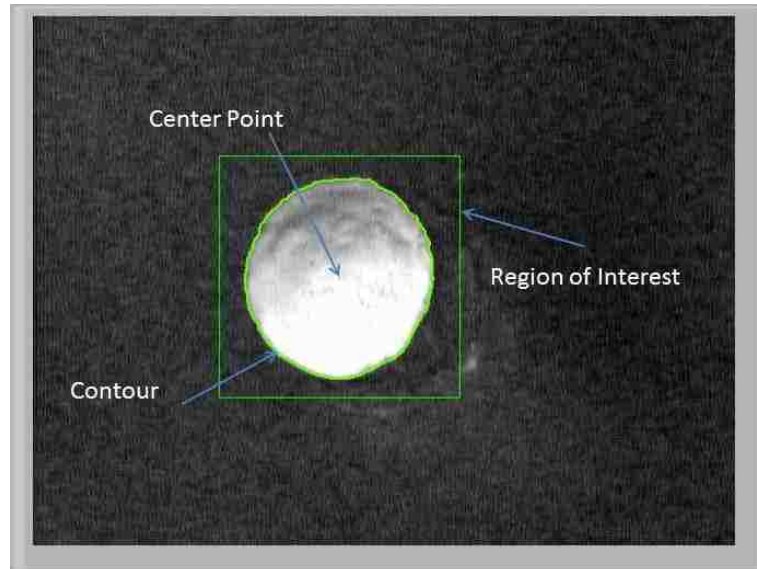


Figure 36 - Labview Image Acquisition Region of Interest

CLOSED LOOP EXPERIMENTS

Building from the previous Matlab Simulink simulations the experimental control laws are built in Labview. As a result of the simulations a PI control law will be used without separately calculating a steady state voltage value based upon the desired location. The control law takes in the current IPMC tip center which has been smoothed out by averaging the previous three values. This should take some of the noise out of the vision acquisition process.

The desired location is then input either by the user or a computer generated trajectory. The position errors are independently calculated and displayed to the users. The PI controller gains are programmable and are input by the user on the front panel. The derivative control was tested however with the noise of the vision acquisition software the system became unstable with large voltage swings caused solely by errors in

the circular curve fit calculation. The Labview simulation uses pixel locations instead of millimeters. The simulations used the displacement and therefore the error in millimeters. As a result the gains from the simulations were converted into the equivalent gains in Labview. These gains were then experimentally varied and validated in the following simulations.

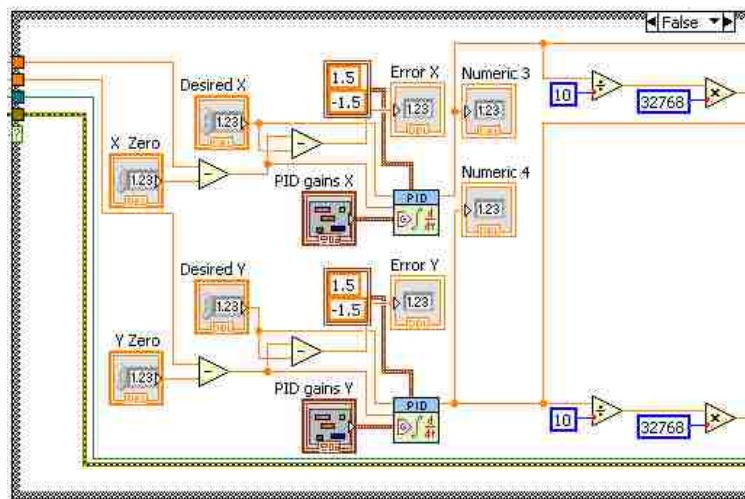


Figure 37 - Labview PI Block Diagram

For the initial tests the IPMC tip is asked to follow a computer generated circular trajectory. This should test the mobility range of the IPMC as well as the ability to maintain a desired location. The tests are conducted in open air with the IPMC placed back in deionized water in-between each test. Each test lasts no more than two minutes to avoid drying out the tube type IPMC. The radius of the circle trajectory is varied while the voltage is limited to 1.5 volts.

For the test the IPMC is placed in the fixture with a white marker at the tip. The background is then blacked out using paper. The Potentiostats are turned on and put into external control mode. The IPMC is centered in the camera field of view and the current center point is input into Labview to zero out the control law. The trajectory generator is activated and the IPMC is asked to immediately track to the circle. This combines a step position input to test the time response and the circle following to test the error values in the control law.

CLOSED LOOP RESULTS

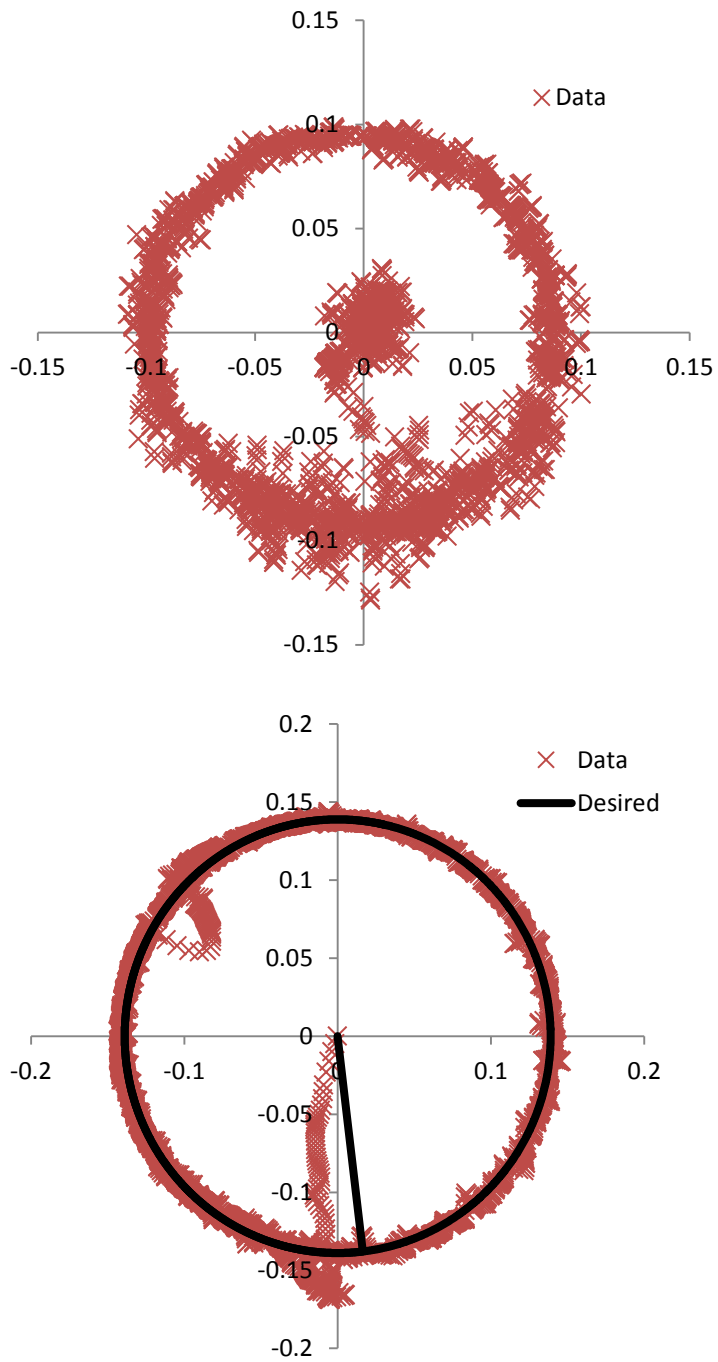


Figure 38 - Experimental Circle with Radii .1 mm and .15 mm

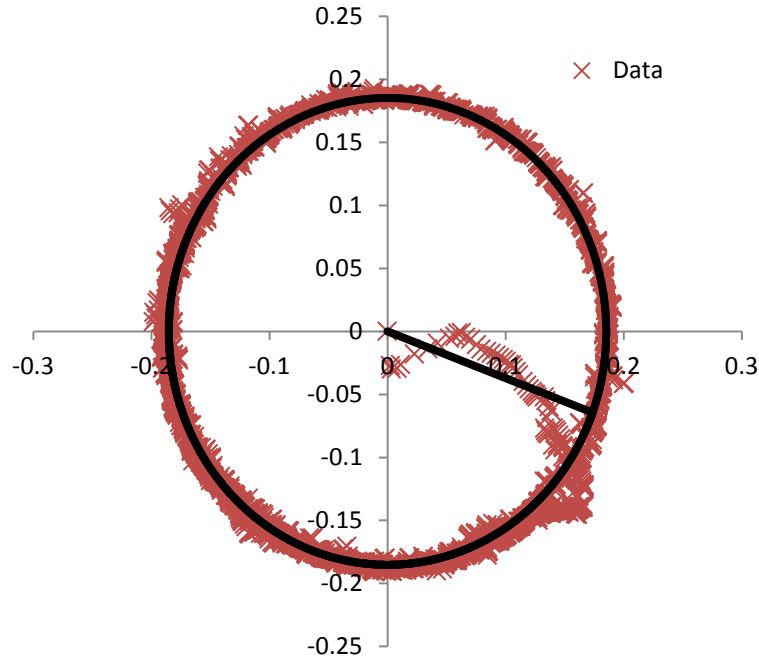


Figure 39 - Experimental Circle Following Data Various Circle Sizes

The IPMC was run through several tests with the tip position following a computer drawn circular algorithm. The diameter of the circle was varied from .2 mm to .4 mm. When the IPMC tip first tracks to the circle a small overshoot is seen. This replicates the results seen in the Matlab simulation. This overshoot is not excessive and is a tradeoff for the speed at which the IPMC tracks the desired trajectory. In these tests the voltage limit was only reached during the initial bending motion and the voltages stayed below 1.5 volts for the remainder of the test.

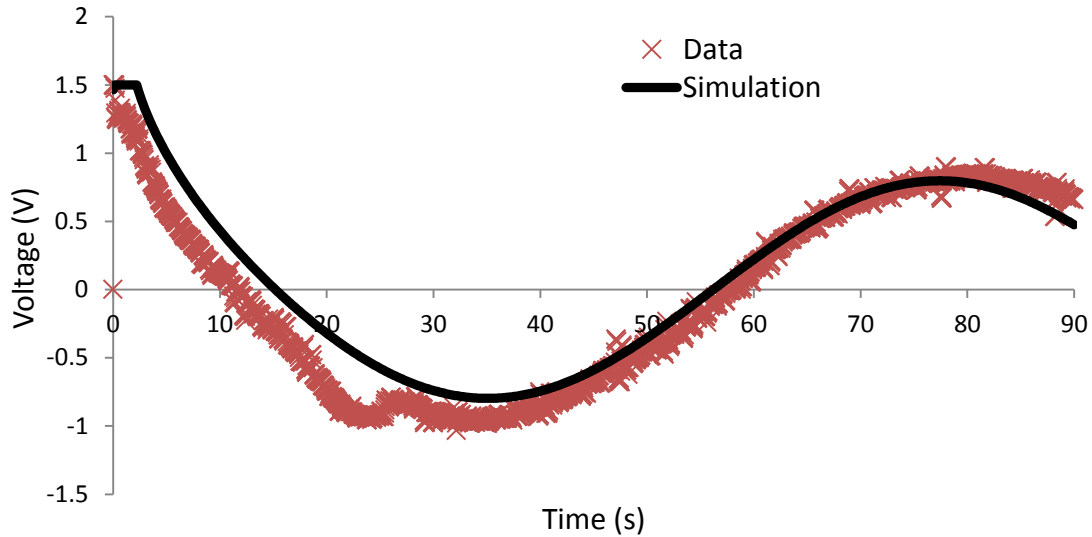


Figure 40 - Simulation Versus Experimental Electrical Data

The figure above is a comparison between the .2 radius circle experimental electrical data and the simulation data presented earlier in the chapter. Both the simulation and the experimental voltages are limited at 1.5 volts. This voltage limit is reached in both cases with the initial motion of the IPMC. The IPMC then follows around the circle where the voltage data remains relatively smooth. Overall the previous simulation has done a very good job at predicting the voltage needed to create this motion. A small deviation in the experimental data is seen around the twenty-five second mark where the IPMC has made a small course correction. It is these unexpected anomalies that the IPMC simulations are not able to anticipate.

For the next test the circular trajectory diameter will be extended to .6 mm. This is near the bending limit of the IPMC sample at 1.5 volts. As a result the voltage limit is

anticipated to have a greater impact. An overshoot of the trajectory in this case is unlikely because the bending rate of the IPMC at this distance will have slowed.

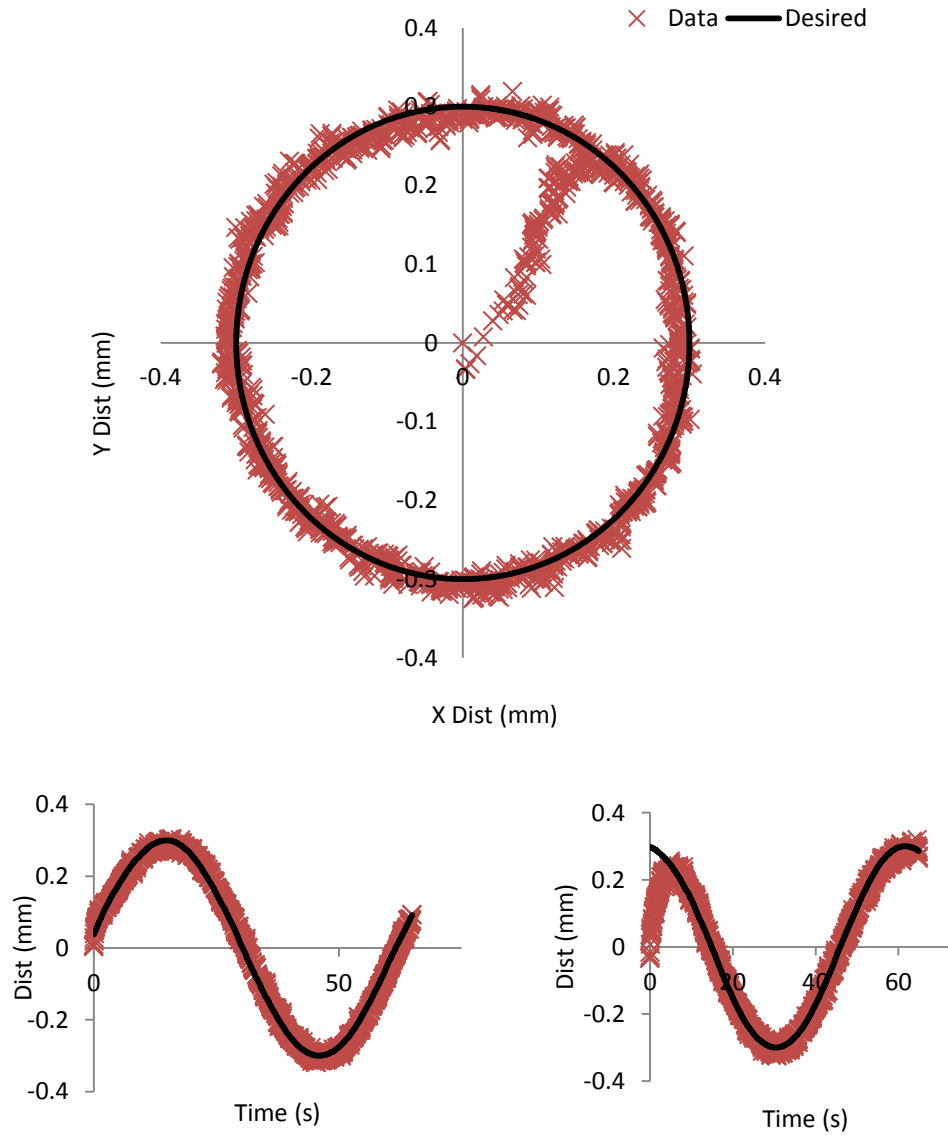


Figure 41 - Figure 8 Closed loop control verification (top) circular path follow (bottom left) x position (bottom right) y position

As seen above the controller is performing well, however the IPMC has some trouble following the circle when the voltage levels are close to their limits. This demonstrates that the IPMC is close to its bending limit at this voltage level. To further investigate this phenomenon the electrical data will be studied.

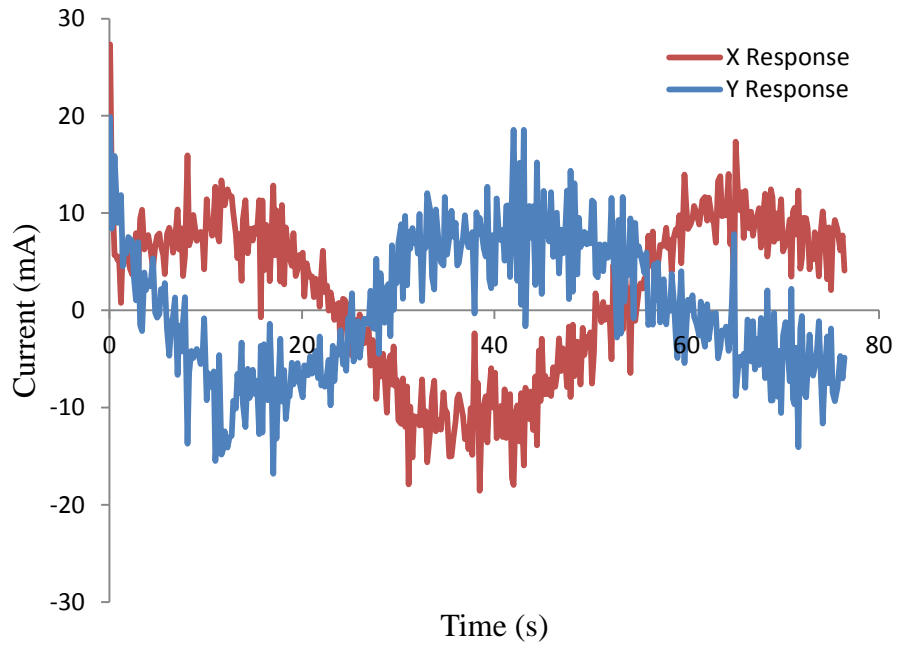
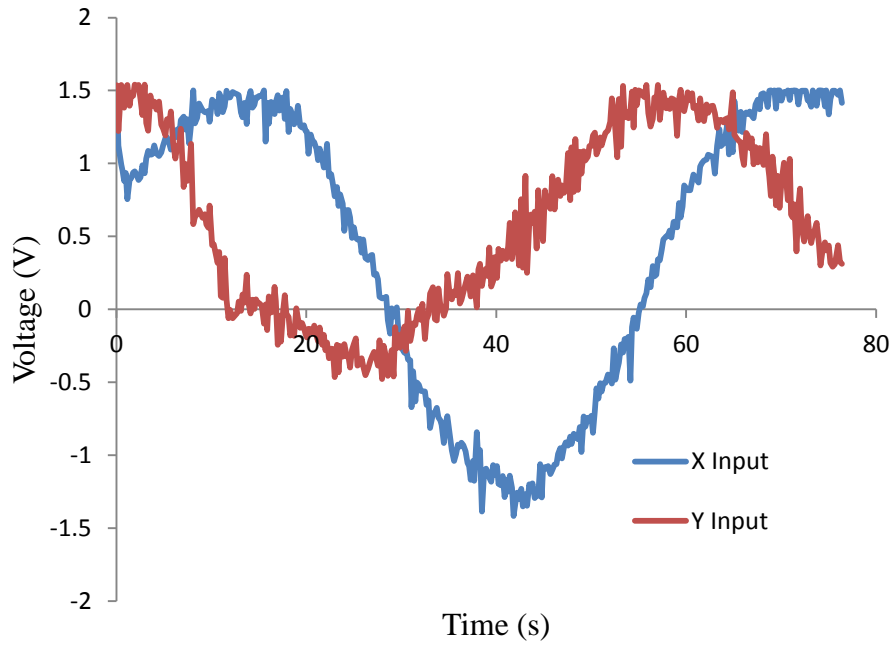


Figure 42 - Electrical Data from .3 mm Radius Circle Following

As seen in the above figure the control law reaches the maximum voltage input on several occasions. The first is when the IPMC is initially bending towards the desired trajectory. This is to be expected because the errors are large and the control law is trying to compensate as quickly as possible. The other occasions are when the IPMC is approaching its maximum X or Y value. This is when the IPMC is asked to bend the farthest and thus requires the most input voltage. As the chart demonstrates this phenomenon is not seen in all occasions but is biased towards one bending direction. When asked to reach the opposite maximum the voltages seen are quite low. This difference has many explanations. One explanation is that the IPMC is not perfectly symmetric. As a result of the manufacturing process the IPMC diameter varies along its length as well as the electrodes themselves being uneven. These manufacturing artifacts would give the IPMC a preferential bending direction from the beginning.

The second explanation is that the IPMC was not perfectly centered or relaxed when the experiment was initiated. This inaccuracy would give the IPMC an artificial zero point that it would actually have to actuate in order to achieve. This slight initial bending would then bias the desired locations for the remainder of the experiment. The reality is that both explanations probably played a part. This experiment was designed to be at the edge of the IPMC's operating ability at 1.5 volts. As a result these limits were reached and the IPMC still performed well.

The IPMC could be operated at a higher voltage level however bubbles were seen when activating the IPMC at a max voltage of 2 volts while in water. When additional samples are available a fatigue and damage study should be conducted. The control law

seems to be able to follow the IPMC tip through a computer input circle quite well. Although this control system is accurate the method for control input is extremely restrictive.

CHAPTER 5

IMPLEMENTATION

The incorporation of functional IPMCs into practical applications is the overall goal of this research. So far a method for designing IPMCs has been explored using the finite element method. The ability to accurately control the tip location has also been demonstrated using the designed control law. With these tools IPMCs can be adapted to an array of real world devices and applications. In order to effectively implement this new technology into conventional devices a few additional attributes have been discussed and examined.

MOUSE CONTROL

As with any new technology there is a desire to decrease the learning time associated with the introduction of a new product in addition to lowering the overall cost. As a result a system was implemented to allow the user to control the IPMC tip location via a standard computer mouse. This allows for a flexibility of motion as well as an input device that the majority of people are already familiar with. This same input can be extended to laptop touchpads and tablet touchscreens. The idea is that the IPMC solution could be plugged in through a standard USB connection and operated on a conventional laptop with no expensive new equipment necessary or lengthy training sessions.

This system is also implemented using a Labview VI. The first problem is getting Labview to accept the mouse motion as an input. To do this the device drivers are installed into the Labview directory and imported into the project folder. Through a specialized VI the location of the mouse pointer and the button status can then be found.

An intuitive control system is then set up. A graphic circle is drawn on the Front Panel of the Labview program and the pixel location of this circle is calculated. When the mouse is within the circle an indicator light is switched on and a flag is set to true. When the left mouse button is depressed a second indicator is switched to true. Only when both the mouse is within this circle and the left button is depressed is this location sent to the control law. When one or both of these indicators are off the IPMC tip location is set to the origin.

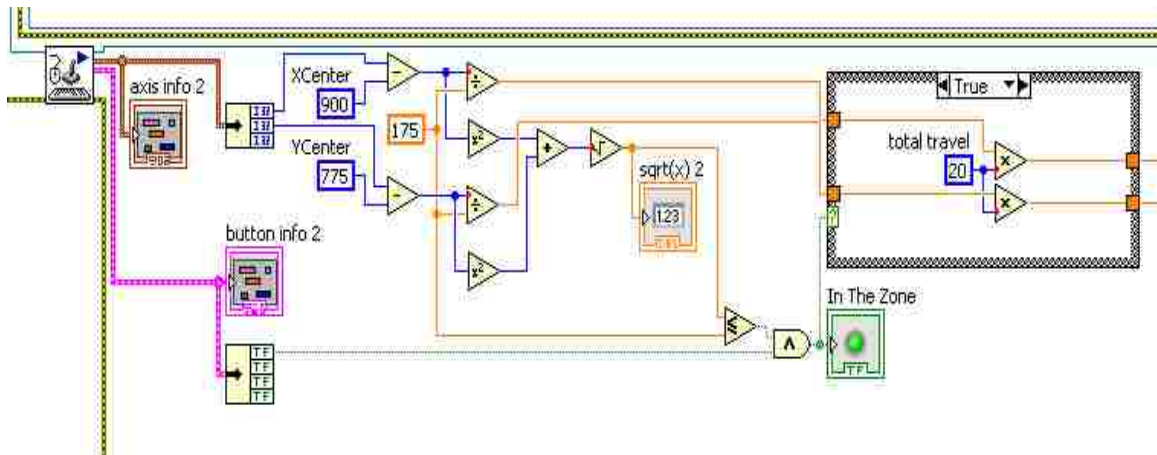


Figure 43 - Block Diagram Mouse Motion Control VI

The mouse pointer location can now be tracked within a circular radius on the screen. This mouse motion must be translated into control voltages. The conversion factor depends upon the maximum voltage set within the VI. The outer radius of the circle is correlated to the maximum tip displacement at the maximum allowed voltage. This distance is varied linearly as the mouse is moved to the center of the circle. The Labview VI “FrontPage” can be seen below.

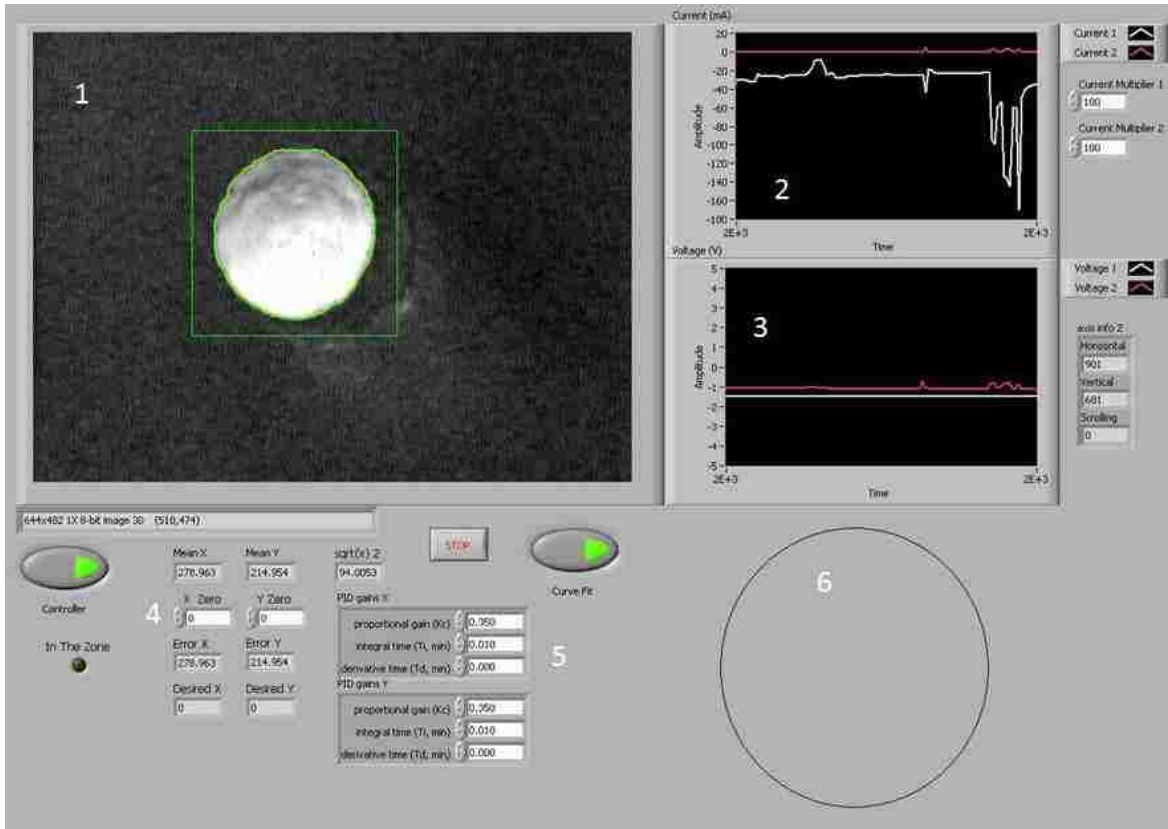


Figure 44 - Labview User Interface

Table 5 - Labview Control Elements

1	Vision Acquisition and Region of Interest
2	Current Monitor
3	Voltage Monitor
4	Center Point Input
5	Controller Gains
6	Mouse input

In addition to providing a familiar interface the mouse interaction provides a vast flexibility of motion for the user. There is no need to translate the desired motions into a complex code; the user need only move the mouse and the IPMC tip will respond. With this flexibility any shape is now possible. For the next test the IPMC is moved through arbitrary trajectories.

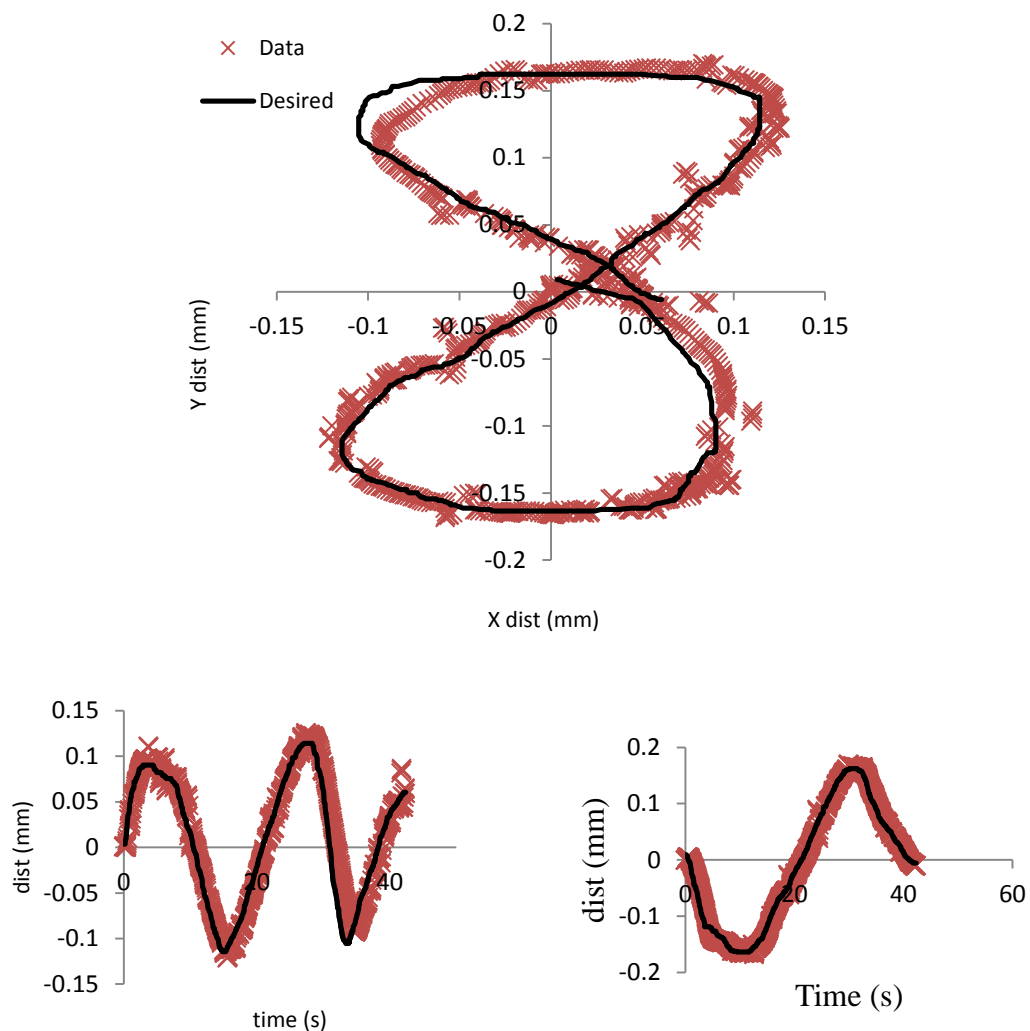


Figure 45 - Closed loop mouse control (top) figure 8 path follow (bottom left) x position (bottom right) y position

As seen the control system still follows the trajectory quite well however, there are a few potential issues. The first is that it is very possible to outrun the IPMC response time. The gains have been set up to provide the fastest response possible without just reaching the voltage limit constantly. As a result it is necessary to move slowly to allow the IPMC time to adjust. This will become a frustrating issue that can be resolved in several ways. The first is to use a smaller sized IPMC that will respond faster. The second is to allow a higher voltage to ramp the IPMC to the desired location. The next potential problem is the variance in location when loading the IPMC into the fixture. The control law still needs to be zeroed out at the IPMC tip starting location. When the IPMC is actuated and then released the IPMC does not necessarily return to the initial starting position. Since all of the motion is generated by a fluid motion there is not a rush of ions to bend the IPMC back to the initial position. Instead the IPMC will relax back to near center. If the IPMC is not in its relaxed state when the tip location is zeroed out it will have a tendency to deform better in a single direction. This can influence the overall error in the system. The next problem addressed is the ability to connect IPMCs to conventional devices.

PERMANENT CONNECTIONS

In order to be effectively utilized in conventional devices the IPMC must be able to be permanently installed into a complex device. In practice the IPMC would not be placed and then removed from its fixture repeatedly. The chance for damage and cross connection would become too high, and quality position control could not be guaranteed.

Instead the IPMC would be permanently mounted and the electrodes would be connected to the device control system. To make these connections techniques for soldering to an IPMC were investigated [46]. As a starting point a handmade wire soldering was performed on the IPMC. First a small bead of solder was placed on the base of each platinum electrode. Then the connection wire was tinned and placed up against the solder bead. Heat was then applied to the outside of the connection wire and a solid connection was established. Using this method a minimal amount of heat was applied to the IPMC. One of the most important requirements while making permanent electrical connections is to maintain the separation between the electrodes. If these electrodes are cross connected the IPMC could no longer be effectively actuated.



Figure 46 - Tube Type IPMC Soldering

The process of soldering the IPMC by hand is quite arduous and is not meant to be a permanent solution. To manufacture these devices at a large scale a new method

must be developed. Towards this end attempts were made to solder these connections using a micro soldering station. UNLV has two K&S 4500 Series manual bonding stations in the clean room in the SEB building. Although these stations have been kept clean they haven't been used in five years. These stations use 50 micron diameter gold solder and soldering is performed underneath a microscope to accurately place the solder. The two stations operate in slightly different ways. The 4526 station uses a metal wedge to place the soldering line. The solder connection is made through three elements; the heat provided by the workholder station, the pressure through the wedge, and an ultrasonic vibration. The 4522 wire station uses an electric spark to form a small ball of solder at the end of the soldering line. This ball is then used as a base to create the pressure needed to perform the connection.



Figure 47 - Manual Wire Bonding Station

Both soldering stations were brought up to a point where they were able to perform bonds onto the test pieces provided by the manual bonder company. These test pieces are ceramics plated with gold in various places. Before attempting to solder to the IPMC using these stations the IPMC must first be dried out. The IPMC is then loaded into the station using a plastic fixture designed for this purpose. Many attempts to perform a soldering connection were made. The full range of pressures and contact times were used as well as raising the workholder temperature. The IPMC seems to flex out of the way of the soldering wedge and no permanent connection could be established. Several tests have been suggested. The first is to chemically plate a layer of gold on the outside of the platinum during the manufacturing process. The second is to use an epoxy to create the initial bonding layer.

The second implementation needed is a connection line that feeds into the hole in the tube type IPMC. One of the main applications for this type of actuator is as an active catheter. For this application the IPMC would replace the conventional plastic tip of the catheter line. This line is used to guide tools such as stents to specific locations or used to administer fluids directly to the needed area. To function in this arena the IPMC needs to be able to be permanently attached to a plastic line. To perform this connection the tube type IPMC was aligned to a plastic tube using a centering pin. This pin was placed through the tube and the hole in the IPMC to ensure that the two were aligned. An epoxy was then applied to both sides of the connection joint and the centering pin was removed.

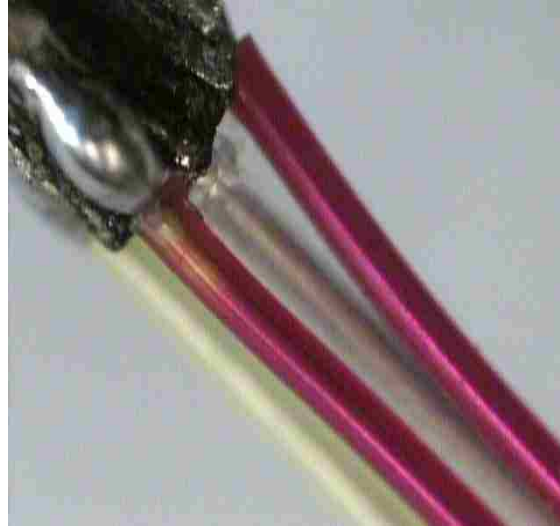


Figure 48 - IPMC Connected to a Plastic Catheter Line

Although this connection was successfully established with limited tube type IPMCs available no tests were performed to characterize the bond. After the connection was made the IPMC and the connection wires were encased in a heat shrink plastic lining to bond the entire system together. Electric connection tests were performed to test the bonds and ensure that no cross connections had been established. Although the electrical connections continued to be isolated limited IPMC bending was seen.

CHAPTER 6

CONCLUSION

The objective of this work was to provide a framework for the integration of tube type IPMCs into conventional devices. To this end two approaches were taken; the first being a finite element model and the second an electro-mechanical based control law. The finite element model coupled three physics packages to model the flow of cations in the presence of an electric field within the IPMC and transform this data into an associated mechanical bending force. Several mesh and bending coefficients were used until the simulation data matched the experimental deflection data. Using this model several simulations were performed to test the effects of tool hole size and Nafion thickness on the overall performance of the IPMC. With these results tube type IPMCs can be tailored to fit real world tasks.

The electro-mechanical model was based on an RC circuit and a set of differential equations linking the motion of charges in the IPMC to the change in curvature. It was found that this model accurately reflects the open loop response of the IPMC to a step voltage input. Using this model a PI controller was designed and implemented in the Labview environment. After several experiments it was found that the control can be used to accurately follow a circular trajectory with the IPMC tip. The control law was then extended to accept the users mouse inputs as the desired trajectory. A mouse was chosen to provide a familiar input device to potential users and to hopefully cut down on training and equipment costs. Several attempts to make permanent connections to the IPMC were made. A successful by hand soldering was accomplished with the isolation of

the electrodes maintained. Attempts to use the K&S manual wire bonding stations were made however no permanent bonds could be achieved. The IPMC was able to be placed in-line with a conventional catheter tube. Control lines were wrapped around the outside and the entire system was encased in a plastic heat shrink line.

FUTURE WORK

There are several areas of the models that could be improved. The first is the overall concentration values found in the Comsol simulations. In the simulation the cations are allowed to be as closely packed as possible without regard to ion size or possible interference from the platinum growth. Some research has explored the possibility of a boundary layer formation defining where the area where there is still some platinum growth and a large cation concentration [47]. This model also includes a packing variable that is related to the size of the actual cations used. The initial deflection in the simulation also needs to be improved. The simulation shows an initial slow bending response where the actual IPMC bends quite rapidly at the beginning.

Several improvements in the electro-mechanical model can also be made. Although the system performs very well as a closed loop system when the system is operated in an open loop configuration the performance is very poor. This highlights a problem or at least an oversimplification in the electro-mechanical model. In many applications it will be difficult to obtain live tracking information of the IPMC tip location. In these applications the IPMC needs to be able to reliably hold its position without a constant feedback. The overall bending magnitude of the IPMC also needs to be addressed. Most of the samples used were nearly two millimeters in diameter. This is a

large diameter for an IPMC. Tests will need to be conducted with actual samples of varying diameter to see if the bending characteristics can be significantly improved.

Work on soldering to a tube type IPMC also needs to continue. Several ideas to improve upon the methods used have been suggested including adding a layer of gold during the IPMC manufacturing and the potential uses of epoxy in establishing permanent connections. With additional flexibility and reliability IPMCs can make a large contribution to society.

REFERENCES

- [1] M. Shahinpoor, K. J. Kim, B. K. Henderson and D. J. Leo, "Sensing capabilities of ionic polymer-metal composites," *SPIE*, vol. 4328, pp. 267-274, 2001.
- [2] Bo-KaiFang, M.-S. Ju and C.-C. K. Lin, "A new approach to develop ionic polymer-metal composites (IPMC)," *Sensors and Actuators*, vol. 137, pp. 321-329, 2007.
- [3] X. Ye, Y. Su and S. Guo, "A centimeter-scale autonomous robotic fish actuated by IPMC actuator," *IEEE Robotics and Biomimetics*, pp. 262-267, 2007.
- [4] K. J. Kim and M. Shahinpoor, "A novel method of manufacturing three-dimensional ionic polymer-metal composites (IPMCs) biomimetic sensors, actuators and artificial muscles," *Polymer*, pp. 797-802, 2002.
- [5] S. Nemat-Nasser and Y. Wu, "Comparative experimental study of ionic polymer-metal composites with different backbone ionomers and in various cation forms," *Journal of Applied Physics*, vol. 93, no. 9, pp. 5255-5267, 2003.
- [6] T. NAKAMURA, T. IHARA, T. HORIUCHI, T. MUKAI and K. ASAKA, "Measurement and Modeling of Electro-Chemical Properties of Ion Polymer Metal Composite by Complex Impedance Analysis," *SICE Journal of Control, Measurement, and System Integration*, vol. 2, no. 6, pp. 373-378, 2009.
- [7] S. J. Lee, M. J. Han, S. JunKim, J. Jho, H. Y. Lee and Y. H. Kim, "A new fabrication method for IPMC actuators and application to artificial fingers," *SMART MATERIALS AND STRUCTURES*, vol. 15, pp. 1217-1224, 2006.
- [8] Jin-Han Jeon, "Selective growth of platinum electrodes for MDOF IPMC actuators," *Thin Solid Films*, vol. 517, no. 17, pp. 5288-5292, 2009.
- [9] K. J. Kim, D. Pugal and K. K. Leang, "A Twistable Ionic Polymer-Metal Composite Artificial Muscle for Marine Applications," *Marine Technology Society Journal*, vol. 45, no. 4, pp. 83-98, 2011.
- [10] J.-H. Jeon, S.-W. Yeom and I.-K. Oh, "Fabrication and actuation of ionic polymer metal composites patterned by combining electroplating with electroless plating," *Composites Part A: Applied Science and Manufacturing*, vol. 39, no. 4, pp. 588-596, 2008.

- [11] S. Nemat-Nasser and J. Y. Li, "Electromechanical response of ionic polymer metal composites," *Journal of Applied Physics*, vol. 87, pp. 3321-3331, 2000.
- [12] M. Shahinpoor and K. J. Kim, "Ionic polymer - metal composites: I. fundamentals," *Smart Materials and Structures*, vol. 10, no. 7, p. 819, 2001.
- [13] T. Wallmersperger, B. J. Akle, D. J. Leo and B. Kroplin, "Electrochemical response in ionic polymer transducers: An experimental and theoretical study," *Composites Science and Technology*, vol. 68, no. 5, pp. 1173-1180, 2008.
- [14] D. Pugal and K. J. Kim, "Finite element simulations of the bending of the ipmc sheet," *SPIE*, vol. 6524, p. 65240B, 2007.
- [15] S. Lee, H. C. Park and K. J. Kim, "Equivalent modeling for ionic," *Smart Materials and Structures*, vol. 14, pp. 1363-1383, 2005.
- [16] Y. Toi and S.-S. Kang, "Finite element analysis of two-dimensional electrochemical-mechanical response of ionic conducting polymer-metal composite beams," *Computers & Structures*, vol. 83, no. 31-32, pp. 2573-2583, 2005.
- [17] J. W. Paquette, K. J. Kim, J.-D. Nam and Y. S. Tak, "An Equivalent Circuit Model for Ionic Polymer-Metal Composites and their Performance Improvement by a Clay-Based Polymer Nano-Composite Technique," *Journal of Intelligent Material Systems and Structures*, vol. 14, no. 633, 2003.
- [18] X. Bao, Y. Bar-Cohen and S.-S. Lih, "Measurements and Macro Models of Ionomeric Polymer-Metal Composites (IPMC)," in *SPIE Smart Structures and Materials 2002: Electroactive Polymer Actuators and Devices*, San Diego, 2002.
- [19] K. Takagi, Y. Nakabo, Z.-W. Luo and K. Asaka, "On a distributed parameter model for electrical impedance of ionic polymer," in *SPIE Electroactive Polymer Actuators and Devices*, San Diego, 2007.
- [20] K. Takagia, T. Osadaa, K. Asakac, Y. Hayakawaa and Z.-W. Luod, "Distributed parameter system modeling of IPMC actuators," in *SPIE Electroactive Polymer Actuators and Devices*, San Diego, 2009.
- [21] D. Pugal, S. J. Kim, K. J. Kim and K. K. Leang, "IPMC: recent progress in modeling, manufacturing, and new applications," in *SPIE Electroactive Polymer Actuators and Devices*, San Diego, 2010.

- [22] S. Nemat-Nassera and J. Y. Li, "Electromechanical response of ionic polymer-metal composites," *JOURNAL OF APPLIED PHYSICS*, vol. 87, no. 7, pp. 3321-3331, 2000.
- [23] W. Yim, M. B. Trabia, J. M. Renno, J. Lee and K. J. Kim, "Dynamic Modeling of Segmented Ionic Polymer Metal," in *IEEE/RSJ International Conference on Intelligent Robots and Systems*, Beijing, 2006.
- [24] S. Gutta, J. Realmuto, W. Yim and a. K. J. Kim, "Dynamic Model of A Cylindrical Ionic Polymer-metal Composite," in *International Conference on Ubiquitous Robots and Ambient Intelligence* , Incheon, 2011.
- [25] G.-Y. Lee, J.-O. Choi, M. Kim and S.-H. Ahn, "Fabrication and reliable implementation of an ionic polymer–metal composite (IPMC) biaxial bending actuator," *Smart Materials and Structures*, vol. 20, no. 105026, 2011.
- [26] H. Nakadoi, D. Sobey, M. Yamakita and T. Mukai, "Liquid Environment-Adaptive IPMC Fish-Like Robot," in *IEEE/RSJ International Conference on Intelligent Robots and Systems*, Nice, 2008.
- [27] X. Tan, D. Kim, N. Usher, D. Laboy, J. Jackson, A. Kapetanovic, J. Rapai, B. Sabadus and X. Zhou, "An Autonomous Robotic Fish for Mobile Sensing," in *IEEE/RSJ International Conference on Intelligent Robots and Systems*, Beijing, 2006.
- [28] Z. Chen, S. Shatara and X. Tan, "Modeling of Biomimetic Robotic Fish Propelled by," *IEEE/ASME Transaction on Mechatronics*, vol. 15, no. 3, pp. 448-459, 2010.
- [29] J. J. Pak, J. Kim, S. W. Oh, J. H. Son, S. H. Cho, S.-K. Lee, J.-Y. Park and B. Kim, "Fabrication of ionic-polymer-metal-composite (IPMC) micropump using a commercial Nafion," in *SPIE Smart Materials and Structures Electroactive Polymer Actuators and Devices*, San Diego, 2004.
- [30] M. Shahinpoor and K. J. Kim, "The effect of surface-electrode resistance on the performance of ionic polymer-metal," *Smart Materials and Structures*, vol. 9, pp. 543-551, 2000.
- [31] J. D. W. Madden, N. A. Vandesteeg, P. A. Anquetil, P. G. A. Madden, A. Takshi, R. Z. Pytel, S. R. Lafontaine, P. A. Wieringa and I. W. Hunter, "Artificial muscle technology: physical principles and naval prospects," *IEEE Journal of Oceanic*

- Engineering*, vol. 29, no. 3, pp. 706-728, 2004.
- [32] U. Deole, R. Lumia and M. Shahinpoor, "Design and test of IPMc artificial muscle microgripper," *Journal Micro-Nano Mechanics*, pp. 95-102, 2008.
- [33] Y. Bar-Cohen, *Electroactive Polymer (EAP) Actuators as Artificial Muscles: Reality, Potential, and Challenges*, Second Edition, SPIE Publications, 2004.
- [34] M. Otis, R. Bemierl, Y. Pasco, H. MCnard, H. Semmaoui, M. Jany and R. Fontaine, "Development of an Hexapod BioMicroRobot with Nafion-Pt IPMC Microlegs," in *International conference of the IEEE EMBS*, Cancun, 2003.
- [35] "MHL Healthcare for the Internet Age," PPM Consult Ltd, [Online]. Available: <http://mhlclinics.com/niobe.html>. [Accessed 26 3 2013].
- [36] "Sensei Robotic System," Hansen Medical Inc., 2013. [Online]. Available: <http://www.hansenmedical.com/international/products/ep/sensei-robotic-catheter-system.php>. [Accessed 26 3 2013].
- [37] "Catheter Robotics INC.," Catheter Robotics, Inc., 2012. [Online]. Available: <http://www.catheterrobotics.com/rcs-main.htm>. [Accessed 26 3 2013].
- [38] J. Lock, G. Laing, M. Mahvash and P. E. Dupont, "Quasistatic Modeling of Concentric Tube Robots," in *IEEE/RSJ International Conference on Intelligent Robots and Systems*, Taipei, 2010.
- [39] T. Shoa, J. D. Madden, N. Fekri, N. R. Munce and V. X. Yang, "Conducting Polymer Based Active Catheter for Minimally Invasive," in *IEEE EMBS Conference*, Vancouver, 2008.
- [40] J. H. Crews and G. D. Buckner, "Design optimization of a shape memory alloy-actuated robotic catheter," *Journal of Intelligent Material Systems and Structures*, vol. 23, pp. 545-562, 2012.
- [41] K. J. K. e. al, *PPA*, No. 61/608,043, filed March 7, 2012.
- [42] E. Shoji and D. Hirayama, "Effects of Humidity on the Performance of Ionic Polymer–Metal Composite Actuators: Experimental Study of the Back-Relaxation of Actuators," *Journal Oh Physical Chemistry*, vol. 111, pp. 11915-11920, 2007.

- [43] R. C. Richardson, M. C. Levesley, M. D. Brown, J. A. Hawkes, K. Watterson and P. G. Walker, "Control of Ionic Polymer Metal Composites," *IEEE/ASME Transactions on Mechatronics*, vol. 8, no. 2, pp. 245-253, 2003.
- [44] S. J. Kim, D. Pugal, J. Wong, K. J. Kim and W. Yim, "A bio-inspired multi degree of freedom actuator based on a novel cylindrical ionic polymer-metal composite material," in *International Conference on Advanced Robotics*, Tallinn, 2011.
- [45] D. Pugal, K. J. Kim and a. A. Aabloo, "An explicit physics-based model of ionic polymer-metal composite actuators," *Journal of Applied Physics*, vol. 110, no. 024904, pp. 084904-1 084904-9, 2011.
- [46] N. N. Pak, S. Scapellato, G. L. Spina, G. Pernorio, A. Menciassi and P. Dario, "Biomimetic Design of a Polychaete Robot Using IPMC Actuator," in *Biomedical Robotics and Biomechatronics*, Pisa, 2006.
- [47] Y. Cha and M. Porfiri, "Charge dynamics of ionic polymer metal composites in response to electrical bias," in *Smart Structures and Materials & NDE*, San Diego, 2013.

CURRICULUM VITAE

Benjamin Mead

6528 Copper Smith Ct, North Las Vegas, NV 89084, (616) 826-7156, Benjamin.Mead@gmail.com

Mechanical Engineer

SUMMARY OF QUALIFICATIONS

- Mechanical engineer with over 4 years experience working in the defense industry as an engineer/project manager
- Managed multi-million dollar projects while working alongside military and government officials
- Master's degree in mechanical engineering with a concentration in dynamic systems and controls
- Active SECRET security clearance; previously cleared TS/SCI SSBI (Oct 2007) with a CI Polygraph (Feb 2008)

EXPERIENCE

University of Nevada Las Vegas – Las Vegas Nevada

Pursuing a Master's degree in mechanical engineering with a concentration in dynamic systems and controls

Research Assistant - Graduate Student

10/11-Present

- Research Assistant working with three-dimensional modeling of flexible Ionic Polymer Metal Composite (IPMC) actuators.
- Designing and developing an experimental closed loop control system for a cylindrical IPMC
- Preparing and presenting project progress reports to senior leadership and to the external funding agency

Merrick and Company/Volt – Las Vegas Nevada

Working virtually as a contract employee in support of the Denver office

Assistant Project Manager

10/10-1/12

- Performed project scheduling for multiple projects, including the development of overall schedule and major milestones
- Maintained project budgets and expenses. Tracked project change orders and adjusted project costs and schedules
- Traveled to job sites as Merrick's representative to government customers and outside contractors

Merrick and Company – Cannon AFB New Mexico

Project manager for the 27th Special Operation Civil Engineering Squadron

Project Manager

04/09-10/10

- Managed over 15 million dollars of new construction and repair projects for the 27th Special Operations Wing
- Executed cradle to grave project management from defining the original project scope to the completion of the project
- Performed the commissioning testing for complex systems including a 12.5 million dollar JP-8 fuel system
- Defined project scope, prepared government cost estimates, and attended negotiations with third-party contractors
- Team lead for a nine person engineering support team consisting of engineers, architects, and construction managers

Lockheed Martin Corporation Mission Service – Northern Virginia

Program provides operations and engineering support for a constellation of on-orbit assets

Associate Systems Engineer

10/07-03/09

- Provided first line identification and troubleshooting for customer assets by executing engineering procedures
- Served as a member of operations team responsible for real-time command and control of complex operating systems
- Interfaced with multiple engineering teams in the response to hardware and software contingencies and in daily operations
- Developed a comprehensive understanding of multiple systems to pass rigorous certification processes
- Obtained additional certifications to serve in a leadership role on the team
- Participated in software testing in support of a new software release

EOSpace Incorporated – Redmond, WA

Designer and manufacturer of the world's lowest optical loss lithium niobate modulators and integrated optical circuits

Engineering Intern

05/06-08/06

- Redesigned environmental testing chamber to increase throughput by 400%
- Attended biweekly design reviews with senior engineer and audited final design documents
- Interacted with machine shops including specifying tolerances, negotiating deadlines, and inspecting finished parts

EDUCATION

University of Nevada Las Vegas - Master of Science in Engineering - Las Vegas, NV

expected graduation 5/2013 Mechanical Engineering with a Dynamic System and Controls concentration

Overall GPA 3.8/4.0 – Member of Tau Beta Pi

Calvin College – Bachelor of Science in Engineering - Grand Rapids, MI

5/2007

Mechanical Concentration with a Mathematics Minor

Overall GPA 3.5/4.0 - Dean's list

Rift Valley Academy – Kijabe, Kenya – High School